BÜŞRA KESİMAL

ATILIM UNIVERSITY 2021

DETECTION OF BLOOD TRACES: SYNTHESIS AND CHARACTERIZATION OF A LUMINOL-TYPE COMPOUND

THE GRADUATE SCHOOL OF NATURAL AND APPLIED SCIENCES
OF
ATILIM UNIVERSITY

BÜŞRA KESİMAL

A MASTER OF SCIENCE THESIS
IN
THE DEPARTMENT OF CHEMICAL ENGINEERING

JULY 2021

DETECTION OF BLOOD TRACES: SYNTHESIS AND CHARACTERIZATION OF A LUMINOL-TYPE COMPOUND

A THESIS SUBMITTED TO
THE GRADUATE SCHOOL OF NATURAL AND APPLIED SCIENCES
OF
ATILIM UNIVERSITY

BY

BÜŞRA KESİMAL

IN PARTIAL FULFILLMENT OF THE REQUIREMENTS
FOR
THE DEGREE OF MASTER OF SCIENCE
IN
THE DEPARTMENT OF CHEMICAL ENGINEERING

JULY 2021

Approval of the Graduate School of Natural and Applied Sciences, Atılım University.

_____

Prof. Dr. Ender Keskinkılıç
Director

I certify that this thesis satisfies all the requirements as a thesis for the degree of the **Master of Sciences in Chemical Engineering and Applied Chemistry at Atılım University**.

_____

Prof. Dr. Şeniz Özalp Yaman
Head of Department

This is to certify that we have read this thesis "DETECTION OF BLOOD TRACES: SYNTHESIS AND CHARACTERIZATION OF A LUMINOL-TYPE COMPOUND" submitted by BÜŞRA KESİMAL and that in our opinion it is fully adequate, in scope and quality as a thesis for the degree of Master of Science.

_____

Prof. Dr. Atilla Cihaner
Supervisor

Examining Committee Members:

Prof. Dr. Murat Kaya
Department of Chemical Engineering,
Atılım University _____

Prof. Dr. Atilla Cihaner
Department of Chemical Engineering,
Atılım University _____

Assoc. Prof. Dr. Merve İçli Özkut
Department of Chemistry,
Ankara University _____

Date: 09.07.2021

I hereby declare that all information in this document has been obtained and presented in accordance with academic rules and ethical conduct. I also declare that, as required by these rules and conduct, I have fully cited and referenced all materials and rules that are not original to this work.

Name, Last Name : Büşra Kesimal

Signature :

ABSTRACT

DETECTION OF BLOOD TRACES: SYNTHESIS AND CHARACTERIZATION OF A LUMINOL-TYPE COMPOUND

Kesimal, Büşra

MSc., Department of Chemical Engineering

Supervisor: Prof. Dr. Atilla Cihaner

July 2021, 59 pages

Luminol is a compound used in many fields, including analytical measurements mainly for forensic science. The synthesis of new luminol-type compounds has gained great importance due to the use of luminol in many fields and also having some disadvantages. In this thesis, a trimeric chemiluminescent 5,8-di(thiophen-2-yl)-2,3-dihydrophthalazine-1,4-dione (T_2B-Lum) compound with pyridazine ring has been studied. After the synthesis and characterization, the chemiluminescence reactions of the compound was investigated in basic medium (0.1 M sodium hydroxide solution) with different oxidants (hydrogen peroxide, potassium permanganate, potassium dichromate). Afterwards, the optical property and chemiluminescence reaction of T_2B-Lum with hydrogen peroxide in alkaline solution in the presence of various metal ions were studied. T_2B-Lum exhibits two absorption bands at 262 and 330 nm in dichloromethane and emits green light at 495 nm when excited. The quantum yield was calculated as 15.11% in dichloromethane when considering the luminol quantum yield is 100%. On the other hand, it was observed that some metal cations, especially copper(II) ions, catalyze the chemiluminescent reaction. It was also observed that the chemiluminescent emission was catalyzed by iron(III) ions.

After this observation, the chemiluminescent behaviors of T_2B-Lum with hydrogen peroxide in alkaline solution were studied in the presence of hemin and blood samples used as catalysts since these samples contain iron ions. Finally, the ion recognition property of T_2B-Lum was investigated. Except for other metal cations (silver(I), cadmium(II), cobalt(II), iron(III), lithium(I), magnesium(II), manganese(II), nickel(II), zinc(II)), it has been observed that T_2B-Lum is mostly sensitive to copper(II) ions with a detection limit value of 2.2×10^{-3} M.

Keywords: Blood detection, chemiluminescence, ion recognition, luminol, thiophene.

ÖZ

KAN İZLERİNİN TESPİTİ: LUMİNOL-TÜRÜ BİR BİLEŞİK SENTEZİ VE KARAKTERİZASYONU

Kesimal, Büşra
Yüksek Lisans, Kimya Mühendisliği Bölümü
Tez Yöneticisi: Prof. Dr. Atilla Cihaner

Temmuz 2021, 59 sayfa

Luminol başta adli-tıp olmak üzere analitik ölçümler dâhil birçok alanda kullanılan bir bileşiktir. Luminolün birçok alanda kullanılması ve bazı dezavantajlara sahip olması nedeniyle yeni luminol-tipi bileşiklerin sentezlenmesi büyük önem kazanmıştır. Bu tezde piridazin halkası içeren trimerik kemilüminesans 5,8-di(tiyofen-2-il)-2,3-dihidroftalazin-1,4-dion (T_2B-Lum) bileşiği üzerinde çalışılmıştır. Sentez ve karakterizasyondan sonra, bileşiğin kemilüminesans tepkimeleri bazik ortamda (0,1 M sodium hidroksit çözeltisinde) farklı yükseltgenler (hidrojen peroksit, potasyum permanganat, potasyum dikromat) ile incelenmiştir. Sonrasında, T_2B-Lum'un optiksel özelliği ve hidrojen peroksit ile beraber alkali ortamda farklı metal iyonlarının varlığında kemilüminesans tepkimesi çalışılmıştır. T_2B-Lum'un diklorometan içerisinde 262 ve 330 nm'de iki soğurma bandı olup uyarıldığında 495 nm'de yeşil ışık yayar. Luminolün kuantum verimi %100 olarak alındığında diklorometan içerisinde T_2B-Lum'un kuantum verimi %15,11 olarak hesaplanmıştır. Diğer bir taraftan, bazı metal katyonlarının, özellikle bakır(II) iyonlarının, kemilüminesans tepkimeyi katalizlediği gözlenmiştir. Ayrıca kemilüminesans ışımanın demir(III) iyonu ile katalizlendiği gözlenmiştir.

Bu gözlemden sonra alkali çözeltide T_2B-Lum'un hidrojen peroksit ile kemilüminesans davranımları katalizör olarak kullanılan hemin ve kan örneklerinin varlığında çalışılmıştır çünkü bu örnekler demir iyonları içermektedir. Son olarak T_2B-Lum'un iyon tanıma özelliği incelenmiştir. Diğer metal katyonları (gümüş(I), kadmiyum(II), kobalt(II), demir(III), lityum(I), magnezyum(II), manganez(II), nikel(II), çinko(II)) dışında, T_2B-Lum'un 2.2×10^{-3} M'lık bir saptama sınır değeriyle bakır iyonuna duyarlı olduğu gözlenmiştir.

Anahtar Kelimeler: Kan tespiti, kemilüminesans, iyon tanıma, luminol, tiyofen.

DEDICATION

To my family

ACKNOWLEDGMENTS

I would like to express my deepest gratitude to the many people who have touched my life and made my life meaningful in various ways. I know that they are my biggest supporters on the way that brought me to this point.

First of all, I would like to thank my advisor Prof. Dr. Atilla Cihaner for his patience, interest, support and willingness to teach his experiences. I am grateful for his advices to complete this master's thesis.

I would like to thank my examining committee members Prof. Dr. Murat Kaya and Assoc. Prof. Dr. Merve İçli Özkut for their interest, valuable ideas and attendance.

I would like to thank Asst. Prof. Dr. Salih Ertan and Dr. Ceren Uzun for their help in the laboratory. It was very valuable to share their experiences with me.

I would especially like to thank my dear friends Bengisu Varlık, Burcu Balcı and Hasan Berk for spending time in the laboratory that I will remember with a smile in the future. I would like to thank members of the Atılım Optoelectronic Materials and Solar Energy Laboratory (ATOMSEL) research group. I am grateful for the nice meetings we spend valuable time with our group. I will never forget these moments in my life.

I would also like to thank Prof. Dr. Ahmet Muhtar Önal from the Department of Chemistry at Middle East Technical University and would like to express my special gratitude to Deniz Çakal for her assistance.

I am very grateful to my family for their support that has brought me to this point. I would like to thank my parents, Nurcihan and Hüseyin for their encouragement and endless love. I say with deep feelings that I would not have succeeded without them.

I would like to express my thanks to my brother Burak and his wife Merve for their support and my niece Defne, who made me smile with her tremendous and lovely energy.

I would like to express my gratitude to Yusuf Burak for his love and the strength he gave me. I sincerely thank him for making me feel good with his support at every moment.

Finally, I would like to thank the Scientific and Technological Research Council of Turkey (TÜBİTAK, Grant Number: 118Z067) for financial support.

TABLE OF CONTENTS

LIST OF TABLES

LIST OF FIGURES

LIST OF SYMBOLS/ABBREVIATIONS

a.u.	Absorbance unit
A.U.	Arbitrary unit
$A_{Y, S}$	Absorption value of compound or sample
$CDCl_3$	Deuterated chloroform
CE	Counter electrode
CL	Chemiluminescence
D-A-D	Donor-Acceptor-Donor
DCM	Dichloromethane
DMF	Dimethylformamide
DMSO	Dimethyl sulfoxide
DNA	Deoxyribo nucleic acid
ECL	Electrochemiluminescence, electrogenerated chemiluminescence
F	Area of the emission spectrum
FTIR	Fourier transform infrared
HRMS	High resolution mass spectrometry
IR	Infrared
n	Refractive index of the solvent
NMR	Nuclear magnetic resonance
PMT	Photomultiplier tube
$QY_{C, S}$	Quantum yield of compound or standard
RE	Reference electrode
S_x	Singlet states
TBAH	Tetrabutylammonium hexafluorophosphate
T_2B-Lum	5,8-di(thiophene-2-yl)-2,3-dihydrophthalazine-1,4 dione
T_2-PA	4,7-di(thiophen-2-yl)isobenzofuran-1,3-dione
T_2-PI-EtHex	2-(2-ethylhexyl)-4,7-di(thiophen-2-yl)isoindoline-1,3-dione
THF	Tetrahydrofuran

TLC	Thin layer chromatography
T_x	Triplet states
UV	Ultraviolet
Vis	Visible
WE	Working electrode

CHAPTER 1

INTRODUCTION

1.1. Electromagnetic radiation

Electromagnetic radiation is energy which is emitted at the speed of light. It contains radio waves, microwaves, infrared (IR), visible (vis), ultraviolet (UV), X-rays and gamma rays [1]. Visible light is one of the types of electromagnetic radiation which is visible to the human eyes. Some forms of electromagnetic radiation are shown in Figure 1.1.

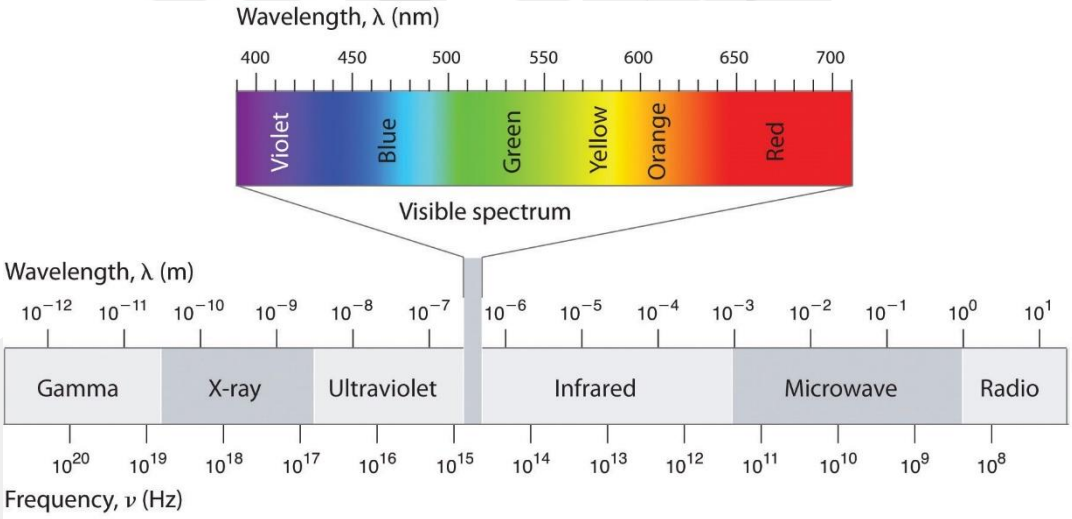

Figure 1.1 The electromagnetic radiation spectrum [2]

1.2. Luminescence

Luminescence is the emission of electromagnetic radiation without changing the temperature of some substances [3]. Luminescence is identified as the emission of electromagnetic radiation in UV (100 nm-380 nm), vis (380 nm - 760 nm) and IR (760 nm-1000 nm) regions [4].

There are several types of luminescence such as chemiluminescence (CL), photoluminescence, bioluminescence, electroluminescence, thermoluminescence, etc. These mentioned types of luminescence are shown in Table 1.1 as based on excitation sources. Luminescence types are named according to the source that triggers the light.

Table 1.1 Classification of luminescence on the basis of the excitation source [3]

Type of luminescence	**Source of excitation**
Photoluminescence	Low-energy photons
Electroluminescence	Electric current
Chemiluminescence	Chemical reaction
Bioluminescence	Biochemical reactions in living organisms
Thermoluminescence	Heating of a substance
Cathodoluminescence	Bombardment of high energy electrons
Radioluminescence	Ionizing radiations
Ionoluminescence	Ion beams
Electrochemiluminescence	Electrochemical reactions
Candoluminescence	Exposure to high temperature
Mechanoluminescence	Release of absorbed light from traps or defects as a result of mechanical stress
Triboluminescence	Breakage of bonds in a material due to rubbing, scratching or crushing
Piezoluminescence	Induced pressure
Fractoluminescence	Breakage of bonds in a material due to fractures
Lyoluminescence	Dissolution of irradiated solute in a liquid solvent
Sonoluminescence	Implosion of bubbles in a liquid due to sound
Crystalloluminescence	Crystallization of a substance
Cryoluminescence	Cooling of a substance

1.2.1. Fluorescence

Fluorescence is one of the forms of photoluminescence. Difference between CL and fluorescence is that their source of excitation is differ from each other. While CL occurs with the chemical reaction, fluorescence radiation is triggered by light. These chemical phenomenons can be explained with the Jablonski diagram as shown in Figure 1.2.

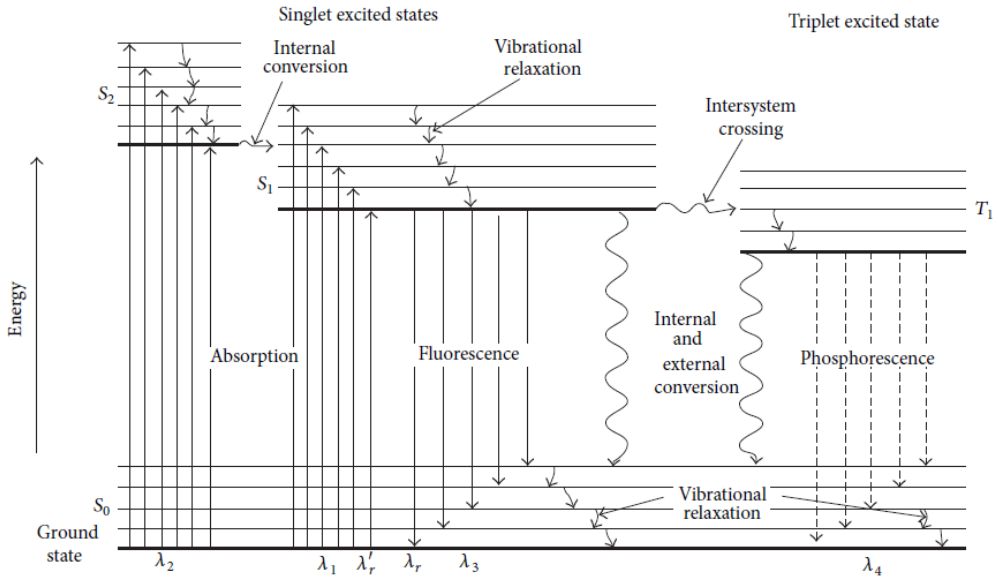

Figure 1.2 Jablonski diagram describing the electronic levels of molecules and possible transitions between different singlet and triplet states [5]

1.2.2. Chemiluminescence (CL)

CL is the emission of light as a result of chemical reaction occurring in the substance. According to the Jablonski diagram, the energy level of the electron increases to excited state as a result of the chemical reaction and when the substance wants to return to its ground state, it emits light with the excess energy.

1.2.2.1. Types of CL Reactions

As seen in the Figure 1.2 for Jablonski diagram, fluorescence and phosphorescence are generated by absorbing UV-Vis light from the electronically excited states (the lowest singlet excited state (S_1) or the triplet excited state (T_1)) to the ground state (S_0) [5]. In general, CL reactions have two basic mechanisms as direct and energy transfer as shown in Figure 1.3.

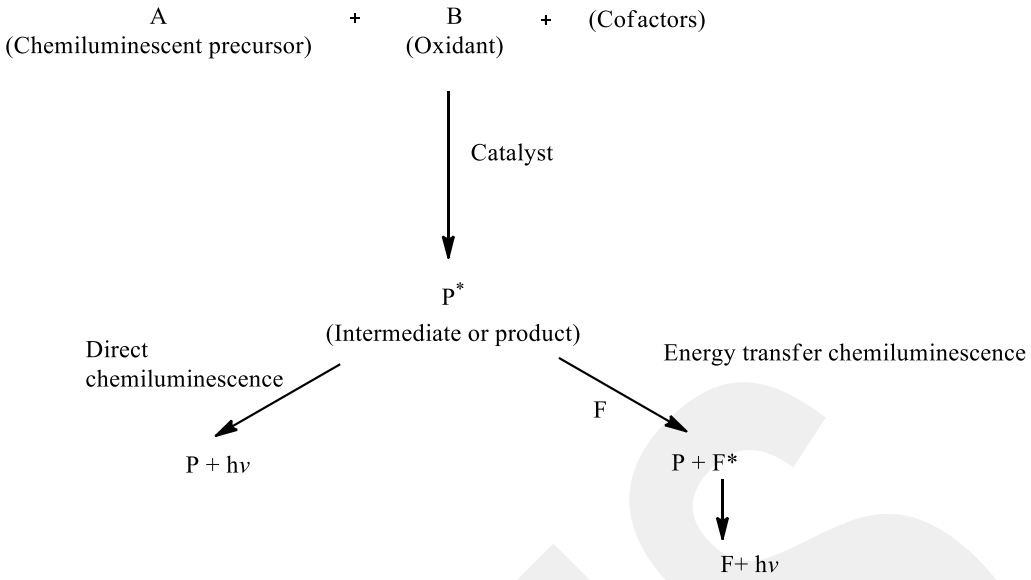

Figure 1.3 Type of CL reactions, P (Product), F (Fluorescing substance) [5]

The two reagents react in the presence of some cofactors and catalyst. As a result, the compound becomes electronically excited state (P^*). After that the compound can follow two different paths. The first way is that the compound which is electronically excited state (P^*) can radiate directly. It is called direct CL. The second way is that the compound which is electronically excited state (P^*) does not radiate itself. It transfers its energy to the substance (F) that will radiate. This matter (F) makes radiance.

1.2.2.2. Historical Evolution of CL Materials

Many compounds have been known to emit visible light for centuries. In the literature, there are glows that excite people since antiquity. Some of those are the aurora borealis, phosphorescence of the sea, luminous animals and insects, phosphorescent wood, etc. as shown in Figure 1.4.

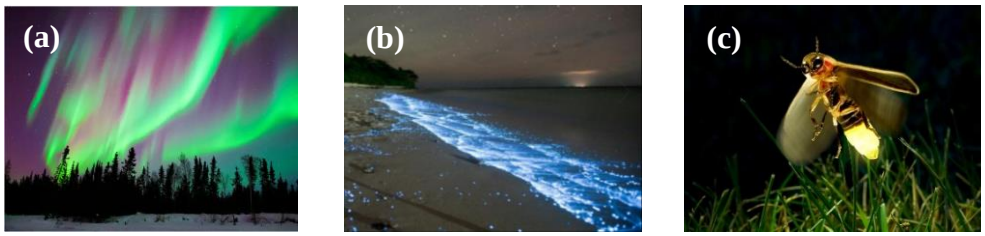

Figure 1.4 Type of luminescent phenomenons: (a) aurora borealis, [6] (b) phosphorescence of the sea [7] (c) firefly [8]

In the literature, Aristotle (384-322 B.C.) seems to be one of the first philosophers to recognize "cold light" in fish and mushrooms. According to early written references, luminescence phenomenon appeared in Chinese literature around 1500-1000 B.C. All of these early observations related on living organisms such as fireflies, bright bacteria, protozoa, sea violets, sea fire worms and dinoflagellates that emit light. This radiation occuring in living organisms is called bioluminescence.

In fact, the early luminescence phenomenons have been generally seen in nature and curiosity has driven human on a long journey.

The first natural phosphorus which was a diamant was shown by Cellini in 1568. In 1652, Italian mathematician Zucchi announced that the Bolonian stone spread more intensely when exposed to bright light. The term "phosphorus" was used in 1669 by Hennig Brand, a Hamburg alchemist who is known as the first scientist to discover a chemical element as phosphor [9]. Human began to create a glowing phenomenon with inspired by nature.

There are some compounds that have CL property such as isoluminol, acridinium esters and dioxetans etc. as shown in Figure 1.5.

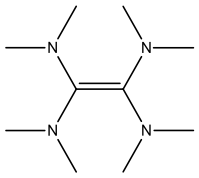

Tetrakis(dimethylamino) ethylene

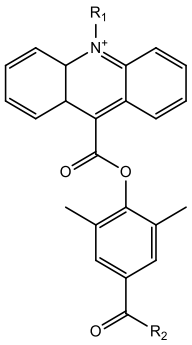

Acridinium ester form

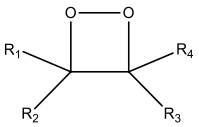

Dioxetan form

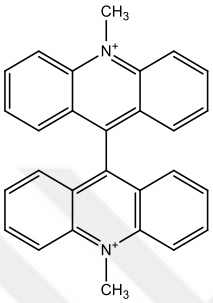

Lucigenin

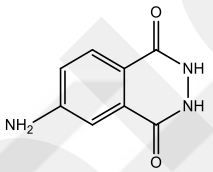

Isoluminol

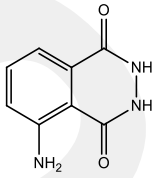

Luminol

Figure 1.5 Some CL compounds

1.3. Luminol

The synthetic substance luminol was discovered in 1853. It was explained by Albrecht in 1928 that luminol (5-amino-2,3-dihydro-1,4-phthalazinedione) has the intense luminescence property associated with alkaline oxidation [9]. The CL effect of luminol was observed on hematin in 1936. Studies on hemin were performed in 1937 and it was reported that luminol would be used in blood detection. In 1939, information about the chemical structure and reaction properties of luminol was found. In 1961, it was found that the luminol excited state was 3-aminophthalate which emits photon. In 1985, the reaction mechanism of luminol in the presence of bloodstains was predicted [10].

CL reactions follow two pathways. These are direct and indirect CL. Luminol follows direct pathway for emission [9].

1.3.1. CL of Luminol

Luminol shows CL property in aqueous alkaline solutions (pH=8-14) that hydrogen peroxide is used generally as an oxidant. Metal ions catalyze the reaction. According to Gillard and Spencer, metal ion complexes react with luminol in aqueous alkaline solutions to form light emission [11]. A possible CL reaction scheme is proposed for luminol in aqueous alkaline solution as shown in Figure 1.6.

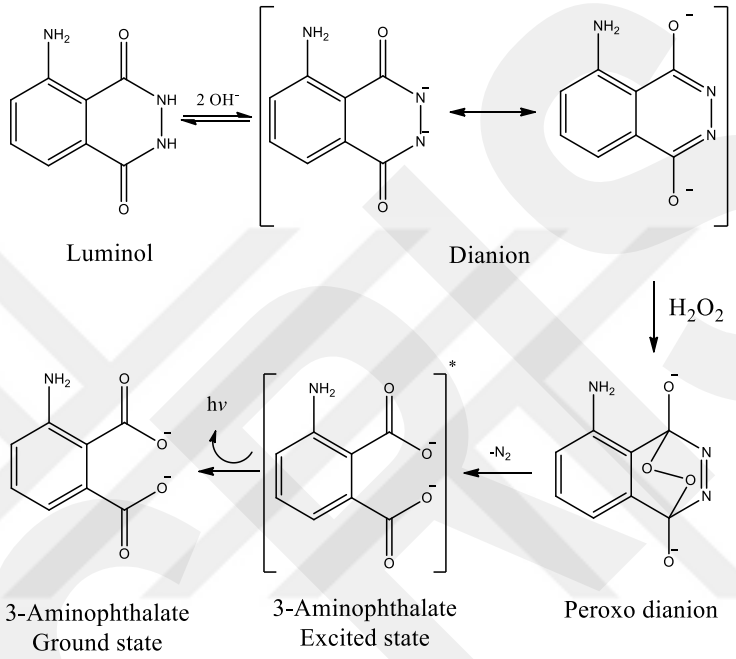

Figure 1.6 A possible CL mechanism of luminol

1.3.1.1. Structural Effects

Earlier studies have revealed that changes in the structure of luminol affect CL emission. Although some compounds are luminol isomer compounds, these compounds do not have CL properties as shown in Figure 1.7.

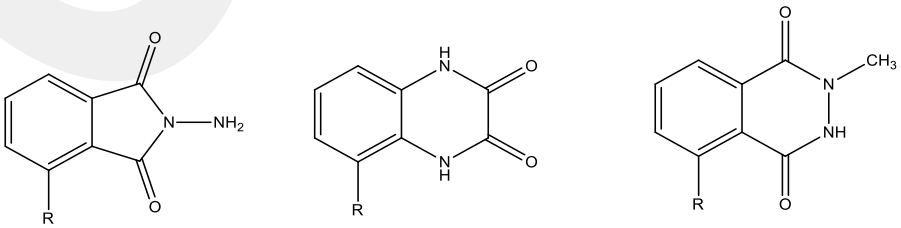

Figure 1.7 Luminol isomer non-CL structures

While changes of luminol in the heterocyclic ring abolish CL, the CL feature was observed in the changes made in the structures in the non-heterocyclic ring. In Figure 1.8, compounds (1) and (2) are more CL than luminol, while compounds (3), (4) and (5) are less efficient [12]. Some groups in the non-heterocyclic ring cause non-bound interactions with the carbonyl group. This interaction causes that compounds are less efficiency than luminol. This is probably due to steric inhibition of resonance.

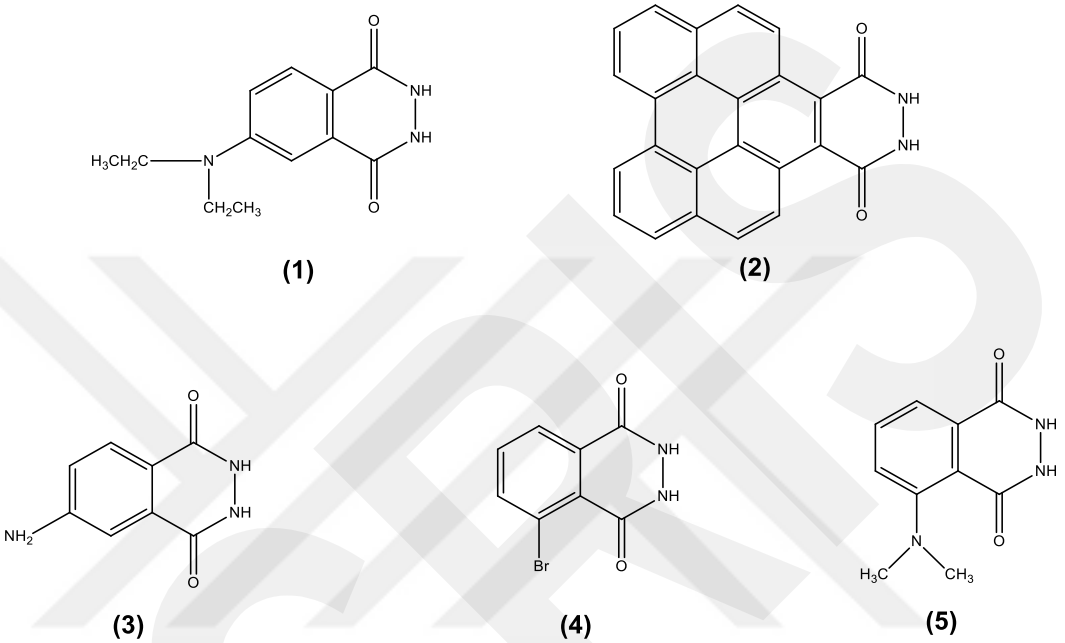

Figure 1.8 Luminol type CL structures

1.3.2. Electrochemiluminescence of Luminol

Electrochemiluminescence (ECL) creates excited states by applying electrical energy to matter. It is also called electrogenerated CL. There is a difference between ECL and CL. The trigger of ECL is electrical voltage. Hence, the radiation can be controlled by the electric voltage.

The first ECL reactions were made in the early 1960s. ECL is the process by which light-emitting type reactions go into electron transfer reactions to create light-emitting excited states. Applying voltage to an electrode in the presence of the light-emitting compound causes light emission. It has been studied in highly purified solvents such as acetonitrile and dimethylformamide (DMF) [13].

There are several possible ECL mechanism pathways for luminol. These pathways may differ depending on the applied potential and the experimental conditions. Luminol converts to the diazoquinone form on the electrode surface by removing protons. These intermediate species convert to the excited state of 3-aminophthalate in the presence of hydrogen peroxide. The excited state of 3-aminophthalate relaxes to the ground state by emitting its energy as blue light (λ_{ECL} = 425 nm). This mechanism is shown in Figure 1.9.

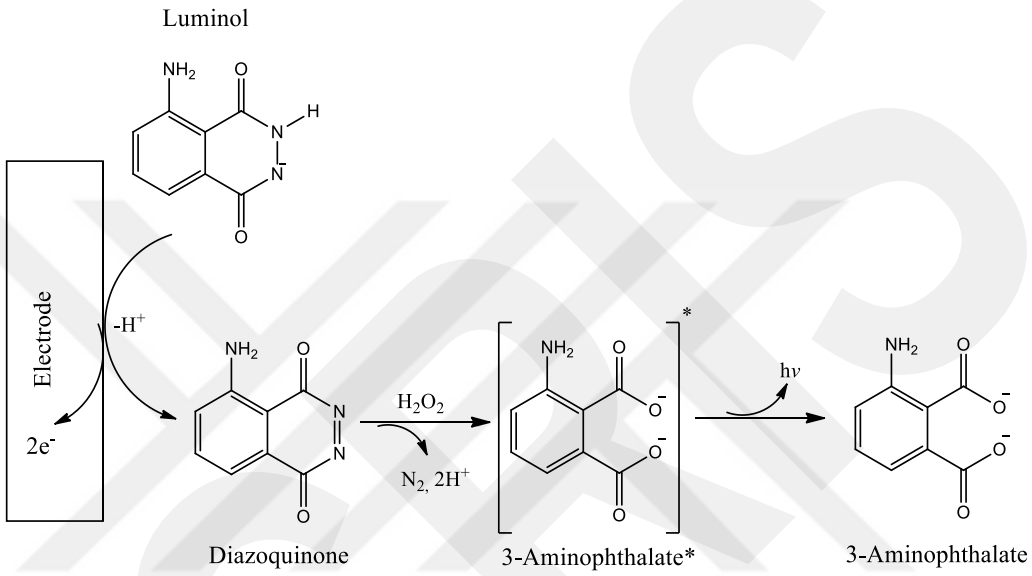

Figure 1.9 A proposed ECL reaction mechanism of luminol

Generally, hydrogen peroxide is an important part of luminol's ECL studies. Hydrogen peroxide can be produced some reactive oxygen species such as peroxide anion (HOO^-) and superoxide radical ($O_2^{\bullet-}$) which accelerate the formation of the excited state of 3-aminophthalate to increase the ECL emission of luminol [14].

1.3.2.1. Cyclic Voltammetry

Cyclic voltammetry is used to determine the electrochemical properties of the materials. The current makes cyclic movements from positive to negative and from negative to positive within the determined potential. Thus, information about the electrochemical properties of the substance is obtained. A cyclic voltammogram provides information about the redox behaviors of the compound, which are the reduction and oxidation peaks. Thus, the reduced and oxidized potentials of the

substance are found [15]. Cyclic voltammetry along with its input and output responses can be seen in Figure 1.10.

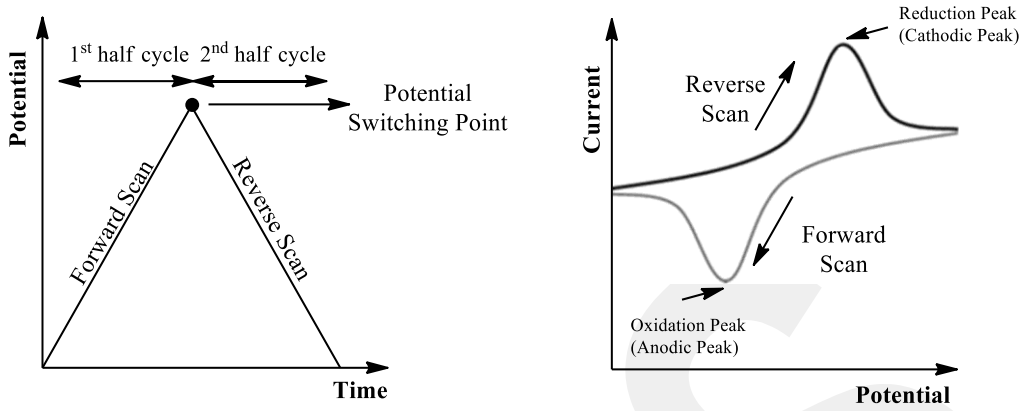

Figure 1.10 Cyclic voltammetry along with its (a) input and (b) output responses [15]

There are five major components for cyclic voltammetry.

i. Working electrode (WE) provides oxidation and reduction of the compound.
ii. The counter electrode (CE) completes the circuit.
iii. Reference electrode (RE) is used to measure potential.
iv. Solution of the chemical to be examined.
v. The RE solution.

The potential of the substance in solution is measured by the potential between the WE and the RE [16].

1.3.3. Application Areas of Luminol

Luminol has many usage areas in the literature. Luminol has been used clinical research such as immunoassay and non-immunoassay applications, biosensors, oncology, nucleic acid assay, gene-based assays, cellular CL, quantification of protein. In addition, it has been used to forensic science to detect blood traces and deoxyribo nucleic acid (DNA) analysis, some pharmaceutical analysis and analysis of a variety of metals [17].

Luminol and their derivatives can be used for the detect of amino acids and peptides, ibuprofen, amphetamine and methamphetamine, histamine, etc. [18].

1.3.4. Luminol in Forensic Science

Luminol is often used to diagnose blood at the crime scene. After experiments with hydrogen peroxide and derivatives from the heme group, the application of luminol in forensic science was first reported in 1937. In studies on luminol, it has been noted that some catalysts increase glow. Luminol compound is in the acyl hydrazide class. It exists in crystalline form. Luminol solutions are highly sensitive to light, strong oxidizing agents, strong acids, strong bases, and strong reducing agents [19].

Hemoglobin is a complex protein that gives red color to the blood. Hemoglobin is found in the erythrocytes of all vertebrates and some invertebrates [10].

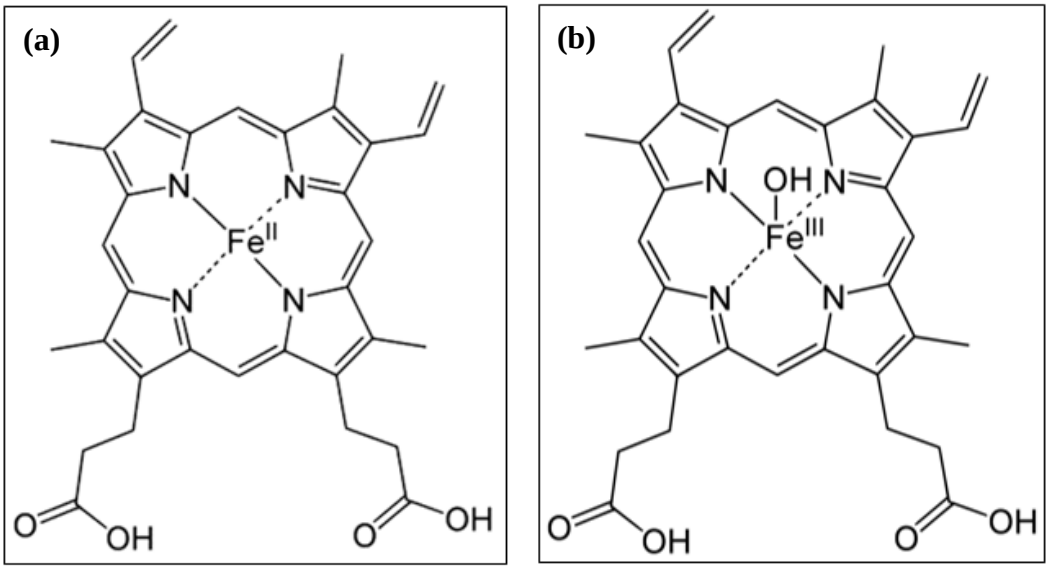

Figure 1.11 Iron binding molecules in blood: (a) hemoglobin in the organism (HEME), (b) hemoglobin outside of the organism (HEMATIN) [10]

Hemoglobin is present in the organism as heme. When it leaves the organism, it undergoes some kind of oxidation and turns into hematin form as can be seen Figure 1.11. Strong CL was observed thanks to hematin form (Fe^{3+}).

The most common evidence found at the crime scene is blood. Luminol test has been accepted as one of the most known method to detect blood traces and frequently used in forensic science by investigators [19].

Figure 1.12 Appearance of blood traces at the crime scene (a) in daylight and (b) dark environment after applying luminol solution to the surface [20]

As seen in Figure 1.12 (a), crime scene findings are not visible with the naked eye in daylight. When luminol solution is applied to the crime scene, it reacts with blood findings and the glow can be seen visually in the dark environment as shown in Figure 1.12 (b). Thus, luminol provides convenience to investigators. However, luminol has some disadvantages. Luminol does not sensitive to only iron ions in the blood. It is sensitive to many metal ions and cleaning products, urine and horseradish. This situation causes misleading results for the crime scene. Moreover, luminol has a destructive effect on DNA and some enzymes [10].

1.3.5. Luminol Type Compounds

Since luminol is used in many areas, it has gained great importance in recent years and new luminol derivative compounds have been synthesized. Some luminol derivative compounds are shown in Figure 1.13.

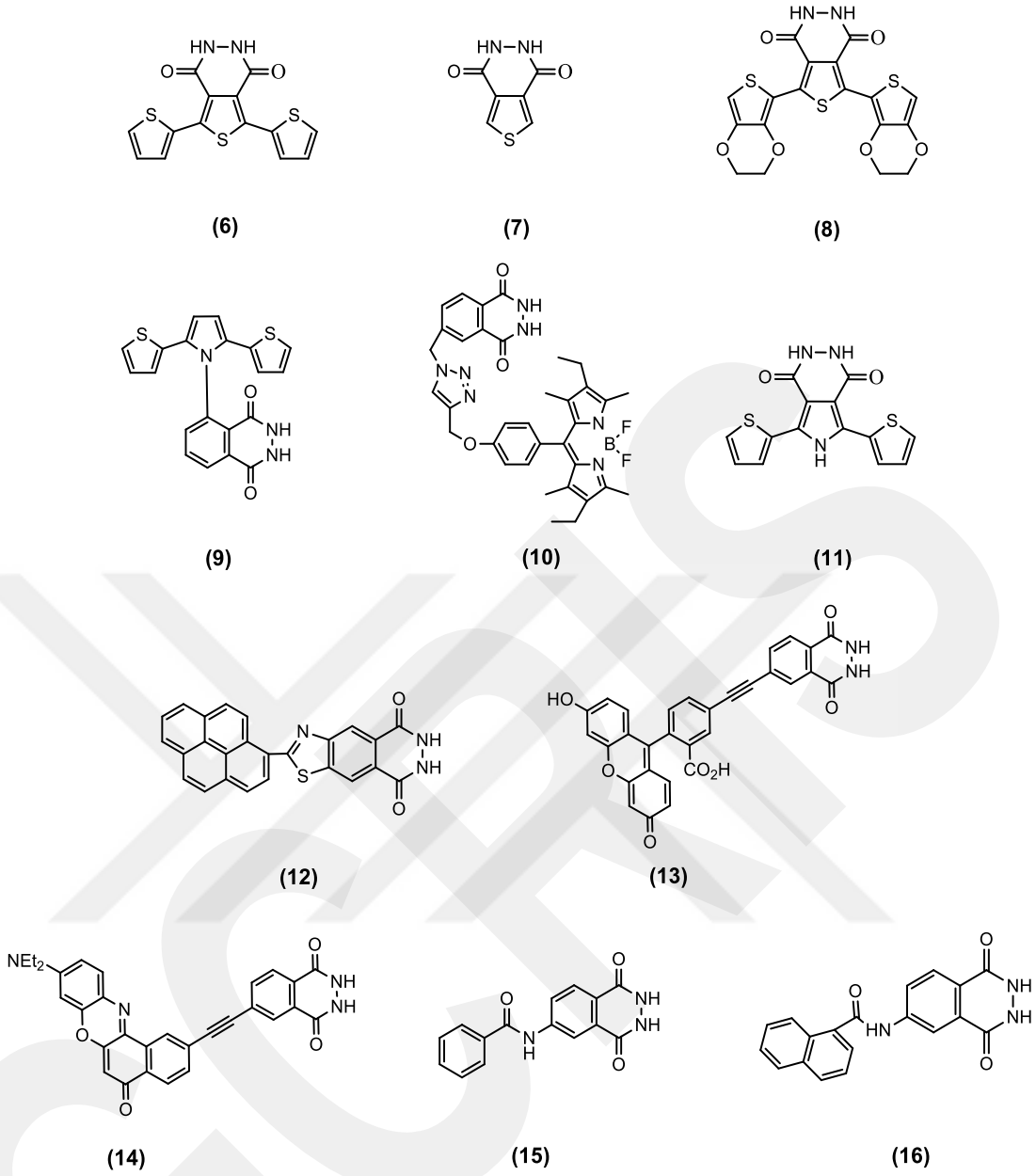

Figure 1.13 Some luminol type compounds: (6) and (7) [21] (8) [22] (9) [23] (10) [24] (11) [25] (12) [26] (13) and (14) [27] (15) and (16) [28]

Whereas luminol is sensitive to many metal ions [29], in Figure 1.13 the substances (6) and (7) are sensitive to Fe^{3+} ions specifically. In addition, Asil et al. carried out polymerization studies for substance (6) as it has a trimeric structure. It is significant for the compound to have a trimeric structure in terms of polymerization.

As stated in the study of Atılgan et al., the compound (8) was catalyzed by Fe^{3+} ion and increased the intensity of the light obtained from the CL reaction. In addition, it has been stated in the study that the compound is sensitive to Fe^{3+} ion.

According to study of Pamuk and Algi, the compound (11) that have a donor-acceptor-donor (D-A-D) trimeric system was used for the detection of Cu^{2+} ion specifically. In the study, it is stated that the D-A-D system has versatility and this trimeric structure can be used in the analysis of different metal ions for different purposes.

In Figure 1.13, the compound (12) and luminol are compared, the relative CL intensity value is much higher for the substance (12) [26].

1.4. Aim of This Study

As seen in the literature, luminol is a compound that use in many areas from forensic-science to analytical measurements and biological and environmental analyzes. However, it has some disadvantages such as destruction of DNA and some enzymes or it is catalyzed some cleaning product such as bleach, faeces, urine or horseradish so luminol gives misleading results. Therefore, synthesis of novel luminol type compounds has gained great importance.

In addition, the compounds with a trimeric structure give the substance versatility property. Trimeric structure of compound provides intramolecular charge transfer so it used many areas such as blood detection to forensic science, analytical chemistry to analyze metal ion, ion recognition property, etc.

Many of the metal ions are quite harmful in biological and environmental processes. Therefore, the development of compounds that enable the selective and sensitive detection of metal ions has gained great importance. In the literature, it has been mentioned that among metal ions, Cu^{2+} is an important element in various biological processes. Cu^{2+} ion is known to cause some diseases such as Alzheimer's, Parkinson's and Wilson diseases, dyslexia, hypoglycemia, and infant liver damage. The target compound could serve as a promising fluorometric probe for the detection of Cu^{2+} ions.

Under the light of these findings, a new trimeric CL compound, namely 5,8-di(thiophen-2-yl)-2,3-dihydrophthalazine-1,4-dione (T_2B-Lum, see Figure 1.14), was synthesized into two steps via D-A-D approach. After characterization, the optical

properties and CL behaviours with H_2O_2 in 0.1 M $NaOH_{(aq)}$ solution in the presence of metal ions were investigated. Also, the sensitivity of T_2B-Lum towards metal ions was studied by following the changes in fluorescence emission of T_2B-Lum.

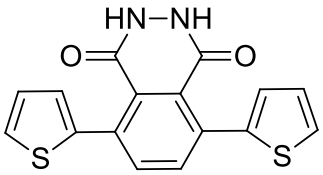

Figure 1.14 Chemical structure of T_2B-Lum

CHAPTER 2

EXPERIMENTAL

2.1. Materials

3,6-dibromophthalic anhydride (>98.0%) was purchased from Tokyo Chemical Industry. 4,7-dibromo-2-(2-ethylhexyl) isoindoline-1,3-dione was purchased from Luminescence Technology Corp. 2-(Tributylstannyl)thiophene (97.0%), bis(triphenylphosphine) palladium(II) dichloride (98.0%), sodium hydroxide (≥98.0%), potassium dichromate (99.9%), potassium permanganate (≥99.0%), benzophenone (99.0%), tetrabutylammonium hexafluorophosphate (TBAH) (≥99.0%) and hexane (≥95.0%) were purchased from Sigma-Aldrich. Hydrazinium hydroxide (80.0%), 1-4 dioxane (≥ 99.0%), hydrogen peroxide (35.0%), sulfuric acid (95.0%-98.0%), deuterated chloroform ($CDCl_3$) (deuteration degree min. 99.8%) and sodium metal (99.0%) were purchased from MERCK. Tetrahydrofuran (THF) (≥99.9%) and glacial acetic acid (99.5%) were purchased from Carlo Erba Reagents. Ethanol absolute (≥99.9%), ethyl acetate (≥99.5%) and dichloromethane (DCM) (≥99.9) were purchased from ISOLAB. Hemin (>98.0%) was puchased from BioChemika.

The metal ions used in the analyzes were purchased from Sigma-Aldrich: $AgNO_3$, $Al(NO_3)_3.9H_2O$, $Cd(ClO_4)_2.xH_2O$, $Co(NO_3)_2.6H_2O$, $Cu(NO_3)_2.3H_2O$, $K_3Fe(CN)_6$, $LiClO_4$, $Mg(NO_3)_2.6H_2O$, $Cl_2MnO_8.xH_2O$, $Ni(NO_3)_2.6H_2O$, $Pb(NO_3)_2$, $(C_2H_3O_2)_2Zn.2H_2O$.

Thin layer chromatography (TLC) and column chromatography were used to purify some synthesized compounds. For this purpose, aluminum plates (20x20, Silica gel 60 F254) were purchased from MERCK and were used for TLC, and silica gel (SiO_2) (0.060-0.200 mm, 60 A) was purchased from Acros Organics and used for column chromatography.

2.2. Instrumentation

2.2.1. Characterization Methods

Nuclear magnetic resonance (NMR) analysis was done by using A Bruker DPX-400 spectrometer. $CDCl_3$ used as a solvent. NMR spectroscopy is a structure illumination method. The compound is placed in a strong magnetic field. The nuclei of some of the atoms in the compound act like a small magnet and absorb electromagnetic rays. This method determines the groups of containing hydrogen and
carbon in a molecule as well as groups adjacent to this group. NMR spectroscopy provides information about the skeleton of compounds.

High resolution mass spectrometry (HRMS) analysis was done by using Waters SYNAPT G1 mass spectrometer. HRMS is a method used to find the atomic composition of substances based on their relative mass.

Fourier transform infrared (FTIR) analysis was done by using Thermo Scientific Nicolet iS10FTIR spectrometer equipped with ATR accessory. FTIR indicates the presence of organic and inorganic compounds in the sample. IR waves cover the range of 12800 ~ 10 cm^{-1} region. However, the area commonly used for IR absorption spectroscopy is 4000 ~ 400 cm^{-1} because this region covers the absorption radiation of most organic compounds and inorganic ions [30].

The melting points of the target compounds were measured with the GALLENKAMP 220/240 V, 50/60 Hz, 50 W device.

Optical studies (absorption and emission/fluorescence) were performed using UV-vis Spectrometer/ Specord S600 and Thermo Lumina Fluorescence Device.

2.2.2. ECL Measurements

Cyclic voltammetry and electrolysis experiments were performed by combining system with Gamry PCI4/300 potentiostat-galvanostat device and photomultiplier tube (PMT) as can be seen Figure 2.1.

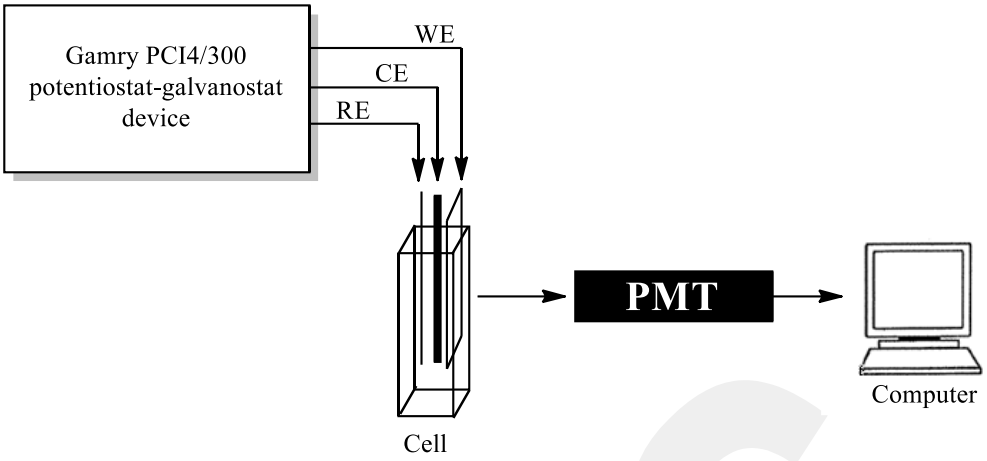

Figure 2.1 Schematic representation of ECL system which include Gamry Potentiostat and PMT.

2.2.3. CL Measurements

Stopped-flow injection system was combined with PMT. This system used in order to measure the CL intensity of the compound. Firstly, responses of T_2B-Lum to different oxidants were observed. Then, some measurements have done in order to observe the effects of metal ions, blood and hemin. The schematic representation of the system in which the analyzes were made is shown in Figure 2.2.

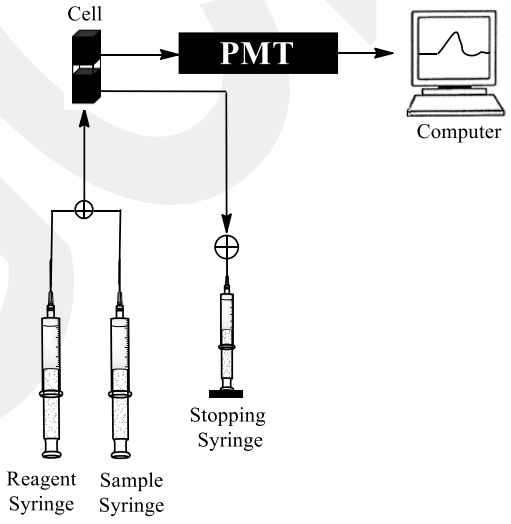

Figure 2.2 Schematic representation of CL measurement system

2.3. Synthesis of Target Compounds

2.3.1. Synthesis of 2-(2-ethylhexyl)-4,7-di(thiophen-2-yl)isoindoline-1,3-dione (T_2-PI-EtHex)

The synthesis scheme of T_2-PI-EtHex compound was shown in Figure 2.3.

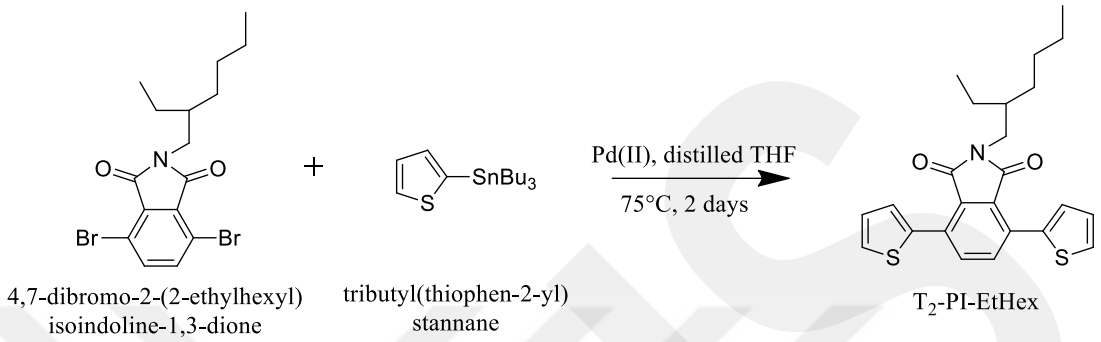

Figure 2.3 Synthesis scheme for T_2-PI-EtHex

4,7-dibromo-2-(2-ethylhexyl)isoindoline-1,3-dione (117.1 mg, 0.281 mmol) was dissolved in distilled THF (2 ml) and it is stirred at 60°C. Then, tributyl(thiophen-2-yl)stannane (230.5 mg, 0.617 mmol) and distilled THF (4 ml) were added dropwise into the mixture and stirred at 60°C. Bis(triphenylphosphine)palladium(II) dichloride (21.65 mg, 0.031 mmol) was dissolved in distilled THF (4 ml) and it was added into the mixture at 75°C after 30 minutes. The reaction was stirred and refluxed at 75°C for 2 days. Reaction followed by the TLC was terminated after 2 days and the mixture was cooled to room temperature. After, most of the THF was evaporated by using rotary evaporator and it was done work-up by using DCM and water to remove impurities. The substance was dissolved in 50 ml DCM and passed into the separatory funnel. After, 50 ml water was poured in separatory funnel. The mixture was shaken and phase formation was observed. DCM phase was taken from the separatory funnel. This process was repeated three times. Organic phase was dried by adding anhydrous $MgSO_4$. After evaporating the solution, the crude product was purified by column chromatography on silica using a mixture of ethyl acetate and hexane. Compound was obtained as light yellow as shown in Figure 2.4: 81.9% yield.

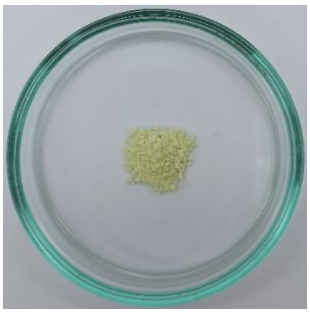

Figure 2.4 Picture of T_2-PI-EtHex

Compound T_2-PI-EtHex: M.p.: 63.7 ± 1 °C. ^{1}H NMR (400 MHz, $CDCl_3$) δ (ppm): 7.80 (s, 2H, ArH); 7.79 (d, 2H, J=4.00 Hz, ArH); 7.51 (d, 2H, J=8.00 Hz, ArH), 7.21 (t, 2H, J=12.00 Hz, ArH); 3.60 (d, 2H, J=8.00 Hz, -CH_2); 1.88, 1.62, 1.31, 1.29 (m, 2H, -CH_2); 0.94 (t, 3H, J=16.00 Hz, -CH_3) (Figure 3.1). ^{13}C NMR (100 MHz, $CDCl_3$) δ (ppm): 167.41; 137.16; 135.69; 132.11; 129.91; 127.64; 127.44; 42.05; 38.04; 30.46; 28.44; 23.78; 22.94; 13.98; 10.34 (Figure 3.2). FTIR (cm^{-1}): 3102, 2961, 2924,2852, 1765, 1691, 1478, 1400, 1362, 1091, 1053, 820, 721, 693 (Figure 3.10). HRMS calculated for $C_{24}H_{25}NO_2S_2$, $[M+H]^+$: 424.1402. Found for $C_{24}H_{25}NO_2S_2$, $[M+H]^+$: 424.1405 (Figure 3.7).

2.3.2. Synthesis of 4,7-di(thiophen-2-yl)isobenzofuran-1,3-dione (T_2-PA)

The synthesis scheme of T_2-PA compound was shown in Figure 2.5.

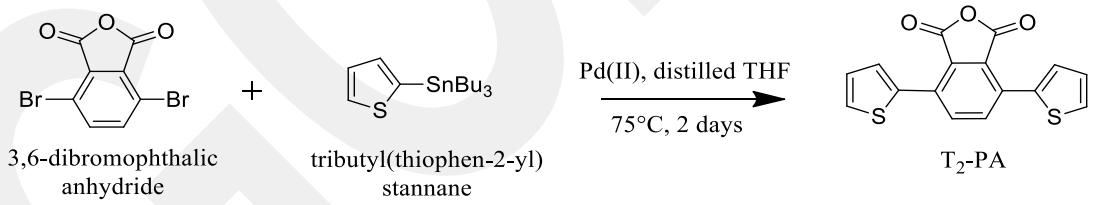

Figure 2.5 Synthesis scheme for T_2-PA

3,6-dibromophthalic anhydride (170 mg, 0.556 mmol) was dissolved in distilled THF (2 ml) and it was stirred at 60°C under Ar atmosphere. Then, tributyl(thiophen-2-yl)stannane (456.2 mg, 1.223 mmol) and distilled THF (4 ml) were added dropwise into the mixture of 3,6-dibromophthalic anhydride at 60 °C. Bis (triphenylphosphine) palladium (II) dichloride (42.9 mg, 0.0611 mmol) and distilled THF (4 ml) were added into the mixture at 75°C after 30 minutes.

The reaction was allowed to be heated and stirred at 75 ° C for 2 days. Reaction followed by the TLC was terminated after 2 days and the mixture was cooled to room temperature. It should be noted that no water was added to the reaction medium and no extraction process was carried out. Otherwise, the phthalic anhydride ring will open. The solution of the reaction mixture, which is THF, was removed by a rotary evaporator. The obtained product is purified by column chromatography by using hexane and then precipitation method is applied using DCM and hexane solvents. Compound was obtained as yellow as shown in Figure 2.6: 39.6% yield.

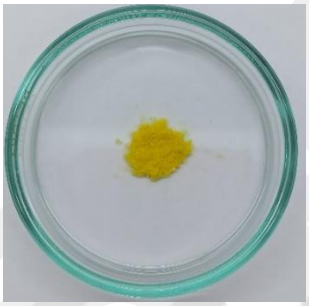

Figure 2.6 Picture of T_2-PA

Compound T_2-PA: M.p.: 179.7 ± 1 °C. ^{1}H NMR (400 MHz, $CDCl_3$, δ, ppm): 7.96 (s, 2H, ArH); 7.88 (d, 2H, J=4.00 Hz, ArH); 7.55 (d, 2H, J=4.00 Hz, ArH); 7.23 (t, 2H, J=4.00 Hz, ArH) (Figure 3.3). ^{13}C NMR (100 MHz, $CDCl_3$, δ, ppm): 160.79; 136.14; 135.01; 133.22; 129.73; 127.62; 127.33; 125.80 (Figure 3.4). FTIR (cm^{-1}): 3115, 2919, 2850, 1818, 1755, 1539, 1476, 1421, 1354, 1275, 1217, 1157, 930, 827, 796, 748, 702, 642 (Figure 3.10). HRMS calculated for $C_{16}H_8O_2S_2$, $[M+H]^+$: 312.9982. Found for $C_{16}H_8O_2S_2$, $[M+H]^+$: 312.9993 (Figure 3.8).

2.3.3. Synthesis of 5,8-di(thiophene-2-yl)-2,3-dihydrophthalazine-1,4 dione (T_2B-Lum)

The target compound was synthesized by two different pathways as shown in Figure 2.7.

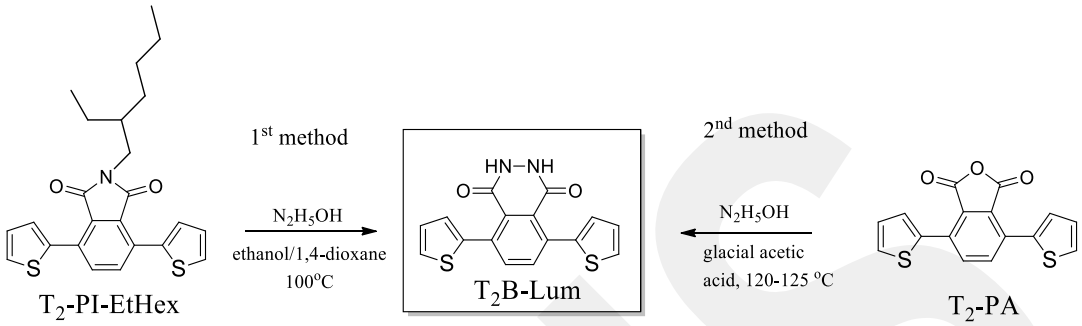

Figure 2.7 Synthesis protocols applied for T_2B-Lum compound

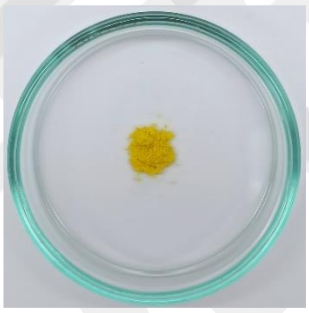

Figure 2.8 Picture of T_2B-Lum

2.3.3.1. First Method for T_2B-Lum

Hydrazine hydrate (500 µL, 0.135 mmol) is added to suspension of T_2-PI-EtHex (57.1 mg, 0.12 mmol) in a mixture of ethanol and 1,4-dioxane (3.5 mL, v/v). This mixture was stirred at 100°C for 2 days with the help of reflux. The reaction was followed by TLC and cooled to room temperature. The corresponding compound was purified by the precipitation method by using DCM and hexane solvents. T_2B-Lum was obtained as a yellow solid: 43.8% yield.

2.3.3.2. Second method for T_2B-Lum

Hydrazine hydrate (573 µL, 0.1548 mmol) was added to suspension of T_2-PA (40.3 mg, 0.129 mmol) in a mixture of glacial acetic acid (2 ml). This mixture was stirred at 120°C with the help of reflux and stirred for 4 hours. The reaction was followed by TLC and cooled to room temperature. The product was purified by the precipitation method by using DCM and hexane solvents. T_2B-Lum was obtained as a yellow solid: 75.9% yield.

Compound T_2B-Lum: M.p.: 134 ± 1 ˚C. ^{1}H NMR (400 MHz, $CDCl_3$) δ (ppm): 7.80 (s, 2H, ArH), 7.79 (d, 2H, ArH); 7.50 (d, 2H, J=4.00 Hz, ArH); 7.20 (t, 2H, J=4.00 Hz, ArH) (Figure 3.5). ^{13}C NMR (100 MHz, $CDCl_3$) δ (ppm): 164.09; 136.64; 136.34; 132.90; 130.24; 129.25; 127.73; 125.71 (Figure 3.6). FTIR (cm^{-1}): 3323, 3216, 3033, 2919, 2852, 2361, 1697, 1646, 1557, 1423, 1367, 1260, 1011, 696 (Figure 3.10). HRMS calculated for $C_{16}H_{10}N_2O_2S_2$, $[M+H]^+$: 327.0261 . Found for $C_{16}H_{10}N_2O_2S_2$, $[M+H]^+$: 327.0262 (Figure 3.9).

CHAPTER 3

RESULTS AND DISCUSSIONS

3.1. Characterizations

^{1}H and ^{13}C NMR spectra of T_2-PI-EtHex in $CDCl_3$ solvent are given in Figure 3.1 and Figure 3.2, respectively. In the ^{1}H NMR spectrum of T_2-PI-EtHex, aliphatic protons appear between 0.00 and 4.00 ppm. While a doublet peak at 3.60 ppm can be attributed to the protons of CH_2 group attached to the N atom, the triplet peaks at 0.90 and 0.94 ppm can be ascribed to $–CH_3$ groups. A multiplet appearing centered at 1.85 ppm is due to the presence of CH group in ethylhexyl chain. On the other hand, aromatic protons can be observed in a range of 7.18 and 7.80 ppm. The peak at 7.29 is due to the $CDCl_3$ solvent.

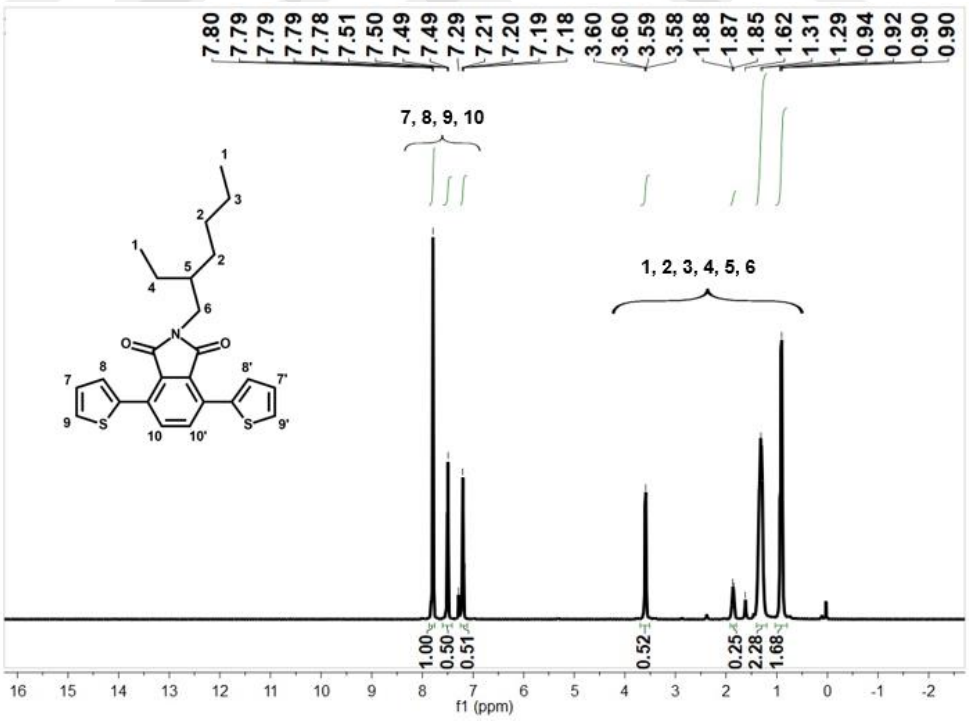

Figure 3.1 ^{1}H NMR spectrum of T_2-PI-EtHex in $CDCl_3$

The carbon atoms in the structure are numbered on the structure given in the Figure 3.2. The numbered carbon atoms were shown on the NMR spectrum. The carbons on the alkyl group are on the right side of the NMR spectrum, and the aromatic carbons are on the left side. $CDCl_3$ solvent represents 3 peaks around 76-77 ppm.

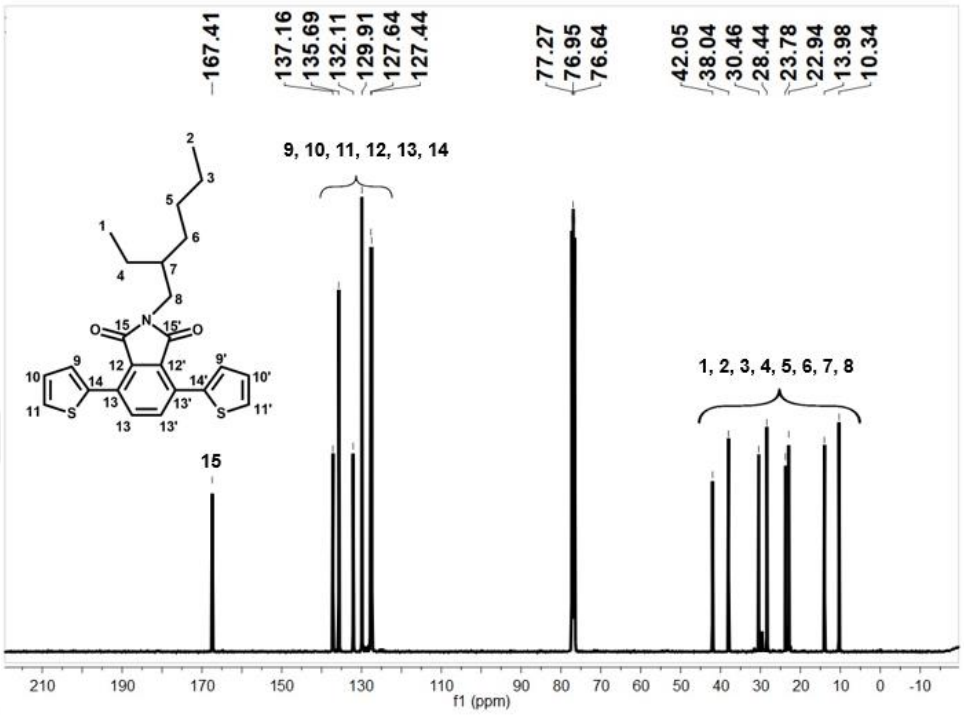

Figure 3.2 ^{13}C NMR spectrum of T_2-PI-EtHex in $CDCl_3$

^1H and ^{13}C NMR spectra of T_2-PA were shown in Figure 3.3 and Figure 3.4. As shown in Figure 3.3, as expected, the spectrum has 4 different signal regions representing the various aromatic protons. Also, T_2-PA has 8 different carbon atoms and they can be easily observed in Figure 3.4. It can be easily concluded that the compound T_2-PA was synthesized successfully based on these two spectra.

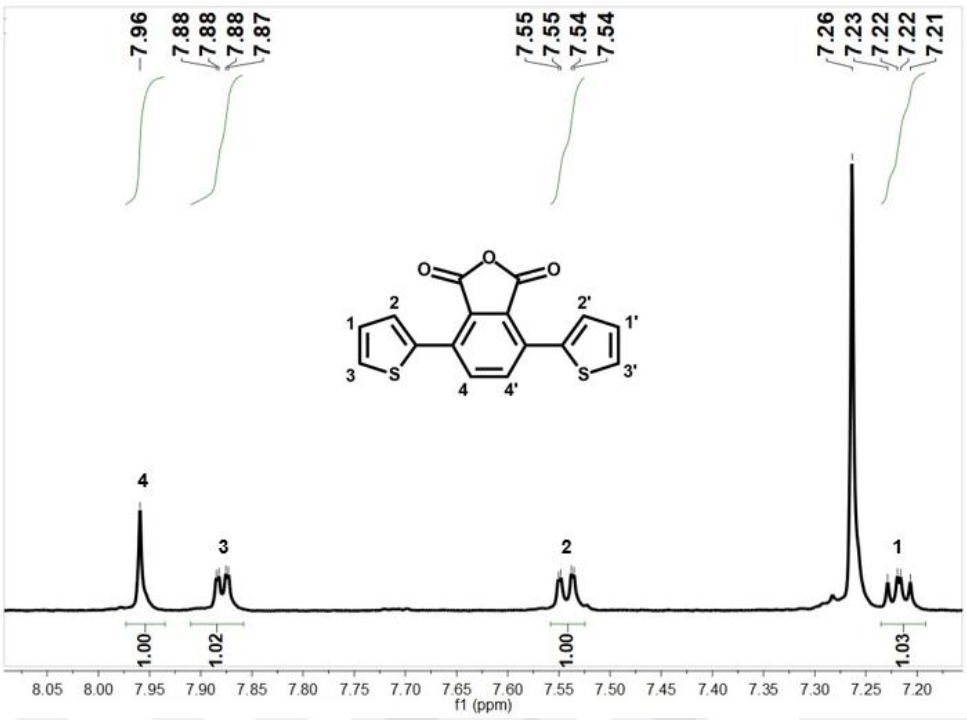

Figure 3.3 ^{1}H NMR spectrum of T_2-PA in $CDCl_3$

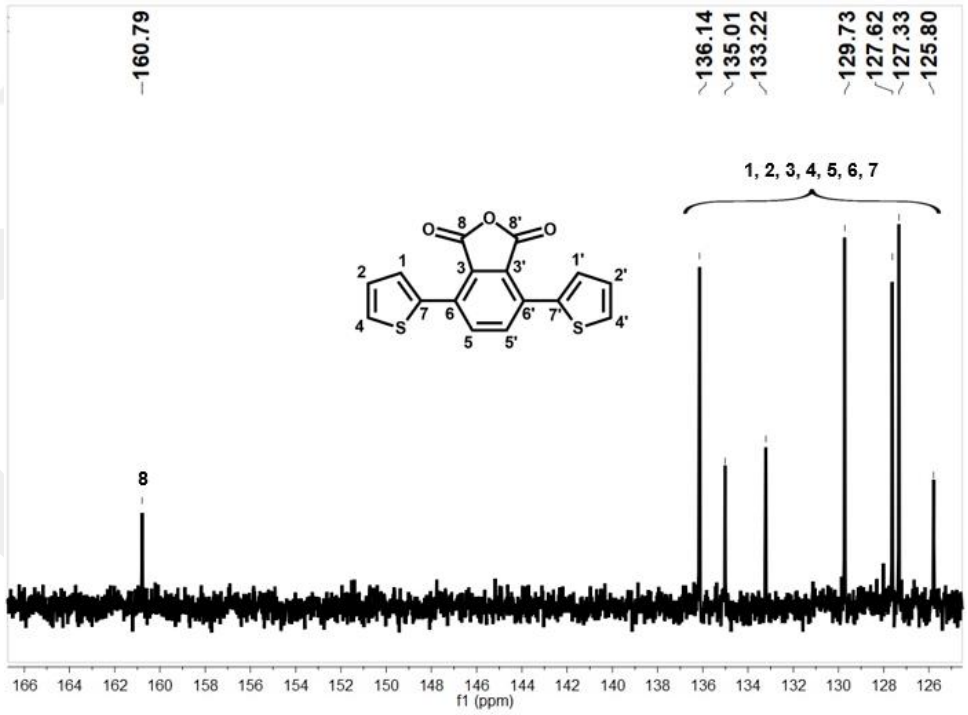

Figure 3.4 ^{13}C NMR spectrum of T_2-PA in $CDCl_3$

Finally, the chemical structure of the compound T_2B-Lum was proved by using ^{1}H and ^{13}C NMR techniques. As shown in Figure 3.5, protons of phenyl group appear at 7.80 ppm as a singlet peak. On the other hand, the protons of thiophene unit are observed at 7.79, 7.50 and 7.20 ppm. Also, the ^{13}C NMR spectrum given in Figure 3.6 supports the structure of T_2B-Lum since it represents 8 different carbon atoms.

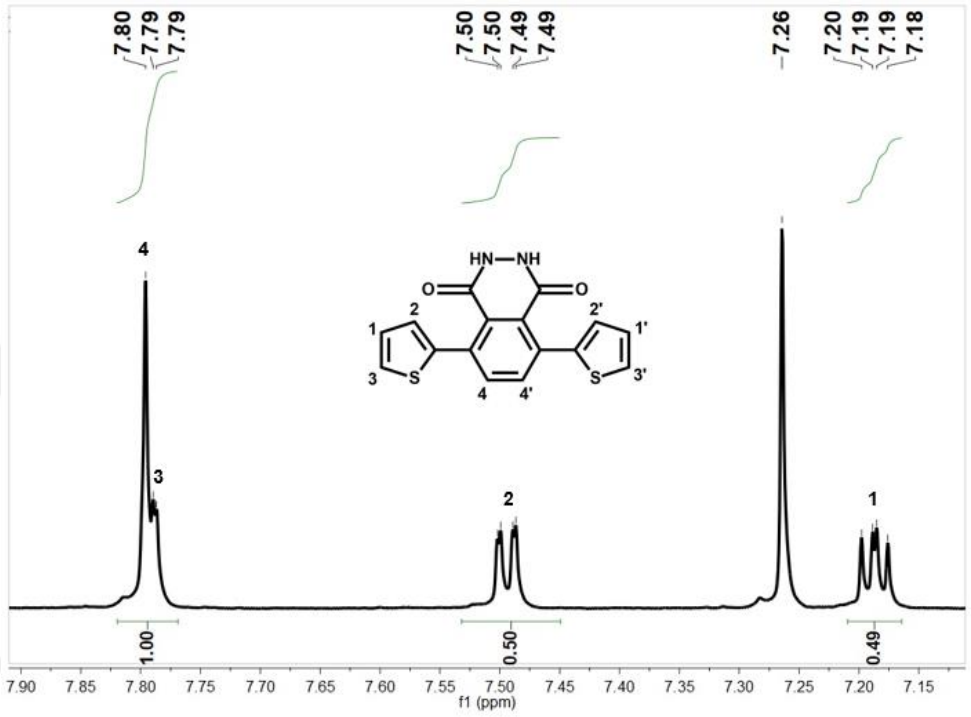

Figure 3.5 ^{1}H NMR spectrum of T_2B-Lum in $CDCl_3$

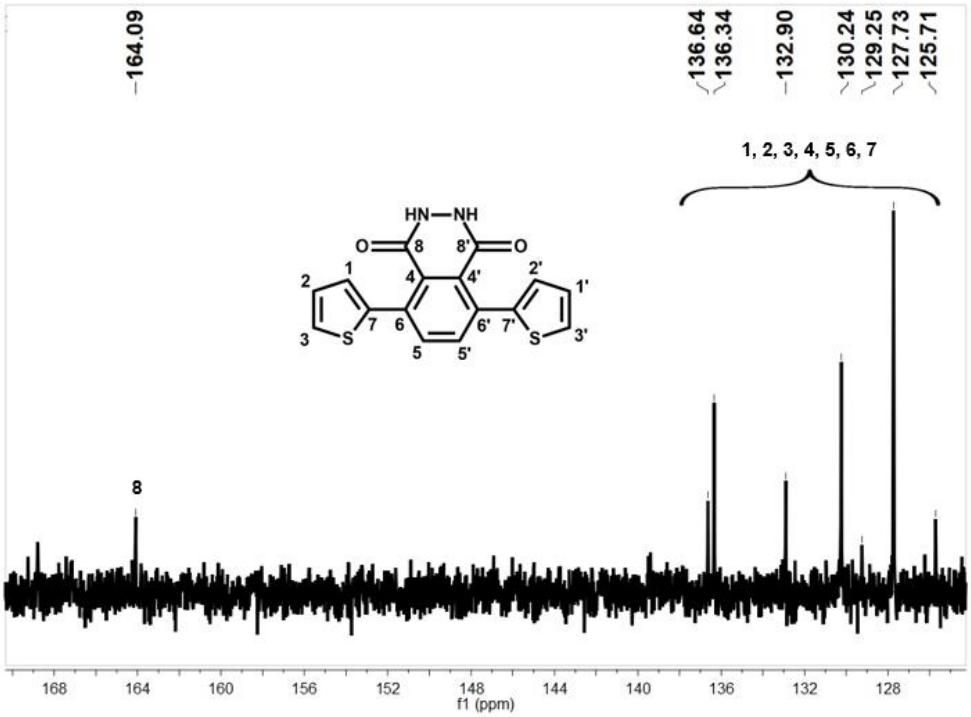

Figure 3.6 ^{13}C NMR spectrum of T_2B-Lum in $CDCl_3$

The HRMS spectra of the T_2-PI-EtHex, T_2-PA and T_2B-Lum compounds were shown in Figure 3.7, Figure 3.8 and Figure 3.9, respectively. Calculated molecular weight values are absolutely confirmed by experimental results.

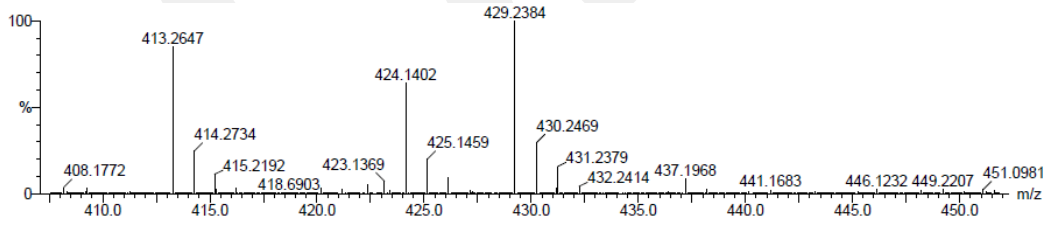

Minimum:				-5.5			
Maximum:		1000.0	5000.0	1000.0			
Mass	Calc. Mass	mDa	PPM	DBE	i-FIT	i-FIT (Norm)	Formula
424.1402	424.1405	-0.3	-0.7	12.5	322.0	0.0	C24 H26 N O2 S2

Figure 3.7 HRMS spectrum of T_2-PI-EtHex

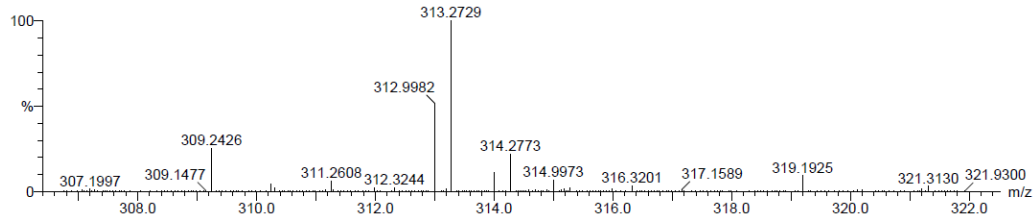

Minimum:				-5.5			
Maximum:		1000.0	5000.0	1000.0			
Mass	Calc. Mass	mDa	PPM	DBE	i-FIT	i-FIT (Norm)	Formula
312.9982	312.9993	-1.1	-3.5	12.5	435.1	0.0	C16 H9 O3 S2

Figure 3.8 HRMS spectrum of T_2-PA

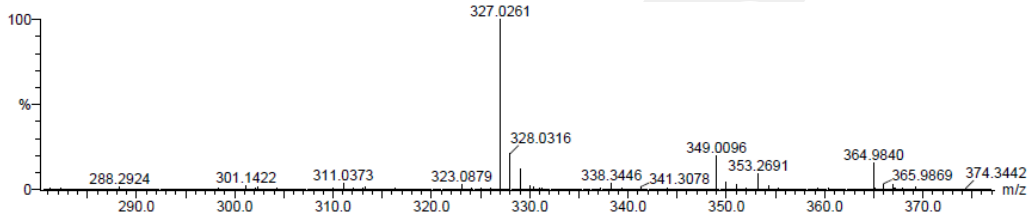

Minimum:				-5.5			
Maximum:		1000.0	5000.0	1000.0			
Mass	Calc. Mass	mDa	PPM	DBE	i-FIT	i-FIT (Norm)	Formula
327.0261	327.0262	-0.1	-0.3	12.5	391.2	0.0	C16 H11 N2 O2 S2

Figure 3.9 HRMS spectrum of T_2B-Lum

FTIR spectra of the synthesized compounds were given in Figure 3.10. The band around 1700 cm^{-1} shows the C=O bond belonging to the carbonyl group for all compounds [31]. The peak at about 3200 cm^{-1} is thought to represent the N-H groups in the pyridazine ring of T_2B-Lum. Para disubstituted aromatic benzene ring shows peak at 790-840 cm^{-1}. In addition, C=C bonds give a peak between 1600 and 1680 cm^{-1}. C and H atom bond peaks are observed between 2850-3000 cm^{-1}.

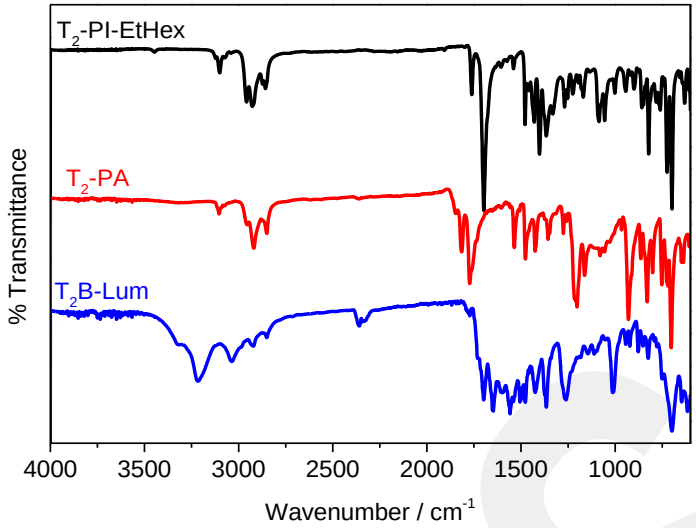

Figure 3.10 FTIR spectra of T_2-PI-EtHex, T_2-PA and T_2B-Lum

3.2. Optical Properties of Synthesized Compound

UV and fluorescence spectra of the compounds are shown in Figure 3.11. Black lines with square shows the absorption and red lines with circle shows the emission of compounds. The presence of at least two main peaks in the absorption band of the synthesized compounds indicates that the compounds have a D-A-D type trimeric structure as can be seen Figure 3.11. The short wavelength peak of absorption band belongs to $\pi \rightarrow \pi^*$ band. The long wavelength peak of absorption band shows the charge transfer between the donor and acceptor units for trimeric structure. Synthesized compounds exhibit a green emission at a longer wavelength due to its conjugated trimeric structure. Absorption and emission peaks are listed in the Table 3.1.

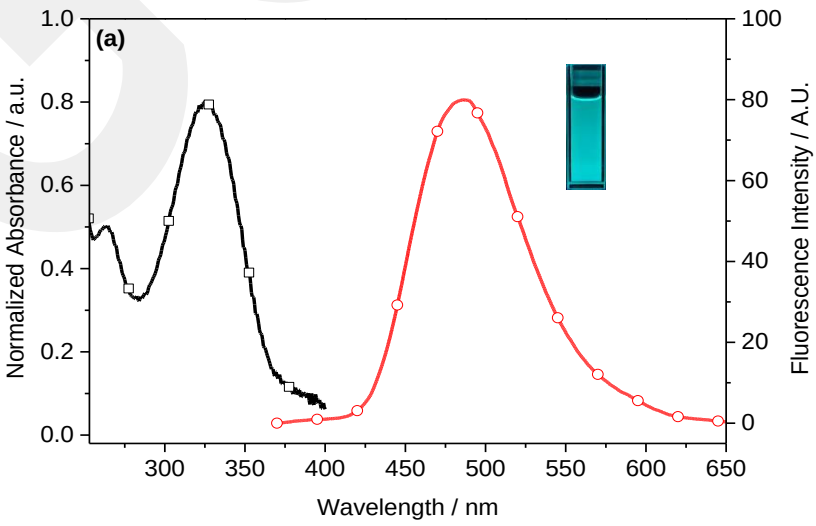

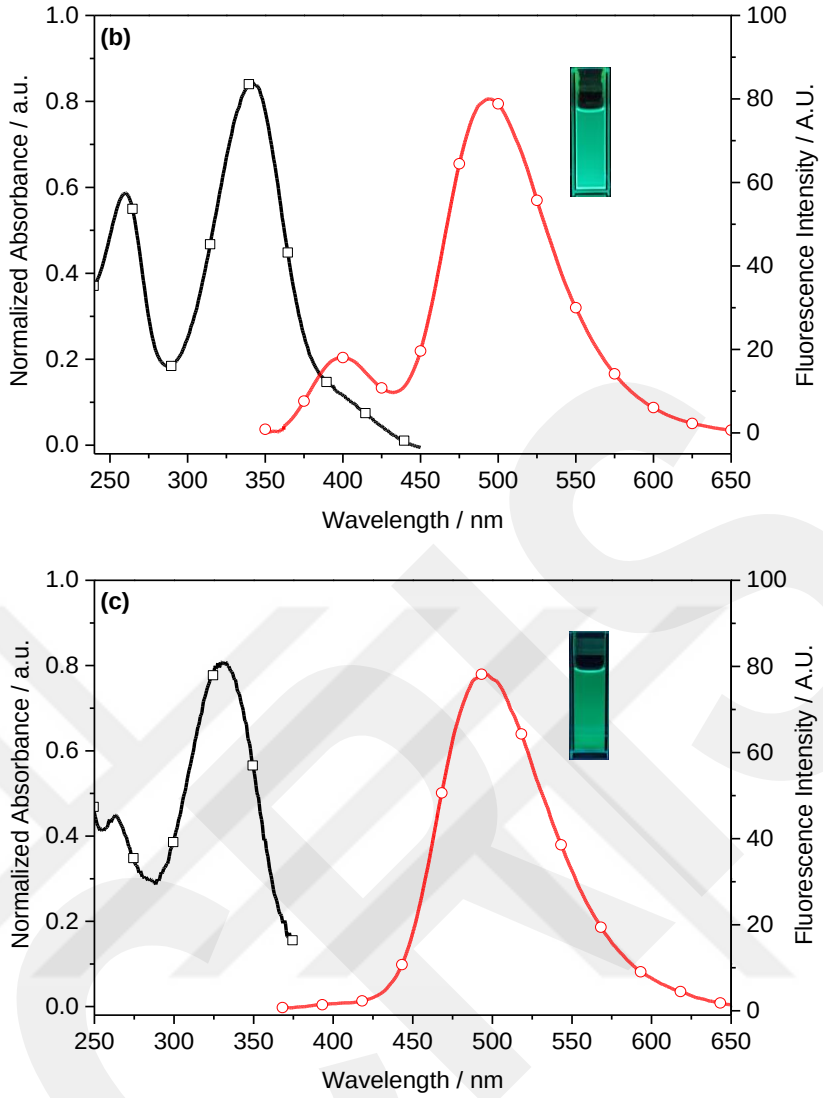

Figure 3.11 Absorbance and emission spectra (λ_{exc}=350 nm) of (a) T_2-PI-EtHex, (b) T_2-PA and (c) T_2B-Lum in DCM

Table 3.1 Absorption and emission wavelengths of T_2-PI-EtHex, T_2-PA and T_2B-Lum in DCM

Compounds	Absorption (nm)	Emission (nm)
T_2-PI-EtHex	264, 325	486
T_2-PA	259, 342	400, 495
T_2B-Lum	262, 330	495

Emission spectra of T_2B-Lum and luminol are given in Figure 3.12. When they excited, the emission band of luminol was observed at 403 nm with blue color and the emission band of T_2B-Lum was observed at 495 nm with green color.

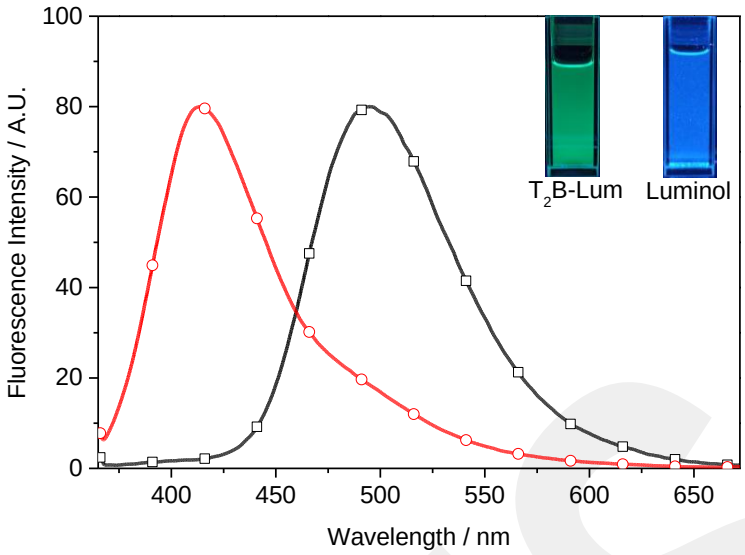

Figure 3.12 Emission spectra (λ_{exc}=350 nm) of T_2B-Lum (black line with square) and luminol (red line with circle) in DCM

3.3. Quantum Yield (QY)

The QY is the determination of the efficiency of photon emission. A certain standard must be used in order to calculate the QY of a compound. The measurements of the compound must be compared with the corresponding standard. There are some standards used in studies: cresyl violet, fluorescein, quinine sulfate, rhodamine 101, rhodamine 6G, rhodamine B etc. In this study, quinine sulfate standard was used. The quinine sulphate standard in 0.1 M $H_2SO_{4\,(aq)}$, at 22°C, the QY is accepted as 58% [32]. The reason for using quinine sulfate is that the absorption spectrum is compatible with T_2B-Lum, as seen in Figure 3.13. All compounds were excited at 350 nm and their emission spectrum was taken.

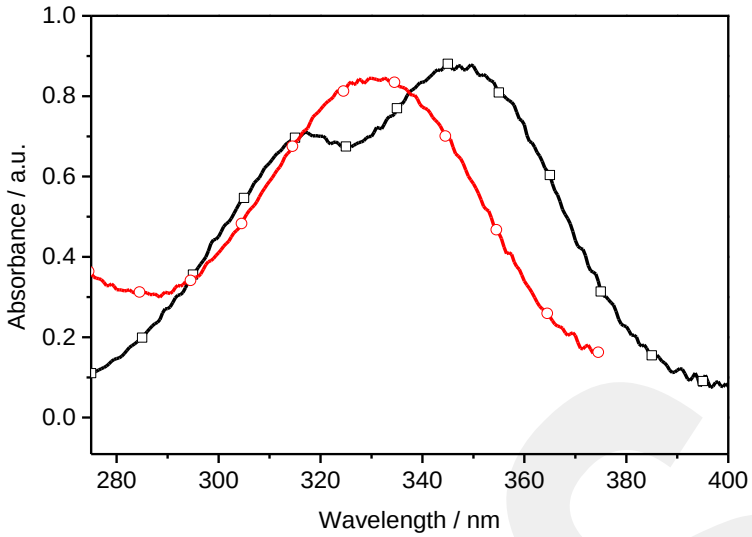

Figure 3.13 Absorbance spectra of (black line with square) quinine sulfate (in the 0.1 M $H_2SO_{4\,(aq)}$) and (red line with circle) T_2B-Lum (in the DCM)

The following equation is used to calculate the QY [33]:

$$QY_C = QY_S \times \left(\frac{F_c}{F_s}\right) \times \left(\frac{A_s}{A_c}\right) \times \left(\frac{n_c}{n_s}\right)^2 \qquad \text{(Eq. 3.1)}$$

"C" and "S" represent compound and standard, respectively.

n = refractive index of the solvent

A = absorption value at the wavelength which the excitation is made and

F = obtained area of the emission spectrum

0.1 M $NaOH_{(aq)}$, DCM and dimethyl sulfoxide (DMSO) solvents were used for T_2B-Lum and 0.1 M $H_2SO_{4\,(aq)}$ was used for the standard. QY were measured as 2.00% in DCM and 1.18% in DMSO as seen in Table 3.2. When the QY of luminol was taken as 100% in order to calculate the QY of T_2B-Lum with respect to luminol, it was observed that it had values of 15.11% in DCM and 6.69% in DMSO as seen in Table 3.3. Emissions of luminol and T_2B-Lum decreased as a result of deprotonation in the basic environment (Figure 3.14).

Table 3.2 QY ($\lambda_{excitation}$ = 350 nm) of compounds obtained in different solvents. Quinine Sulphate Standard (in 0.1 M $H_2SO_{4\,(aq)}$) QY = 58% [32]

Compounds	DCM	DMSO	0.1 M $NaOH_{(aq)}$
T_2B-Lum	2.00	1.18	0.35
Luminol	13.24	17.63	0.02

Table 3.3 QY ($\lambda_{excitation}$ = 350 nm) of the compound relative to luminol (considering the luminol QY as 100%)

Compounds	DCM	DMSO
T_2B-Lum	15.11	6.69
Luminol	100	100

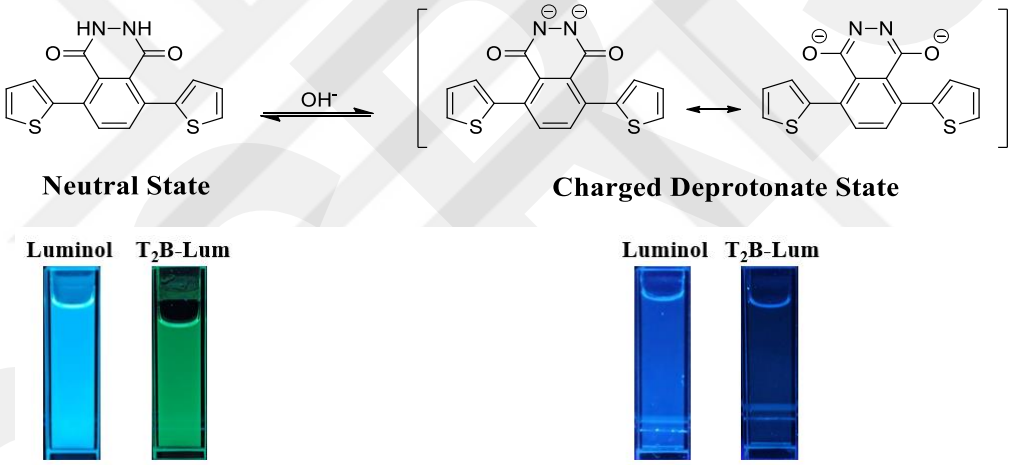

Figure 3.14 Pictures of the luminol and T_2B-Lum at neutral state (in DMSO) and basic condition (in 0.1 M $NaOH_{(aq)}$) charged deprotonated state under UV lamp (365 nm)

The reason for the low QY of the T_2B-Lum can be steric hindrance of resonance [12, 34]. It is thought that there is a non-bonding interaction between the oxygens in the carbonyl group and the electron donating group. Arabacı's study showed that there is a 53° dihedral angle between the donor and acceptor units of T_2B-Lum. The dihedral angle disrupts the planarity and therefore the QY of T_2B-Lum is lower than luminol [35]. T_2B-Lum conformations from the side view are shown in Figure 3.15.

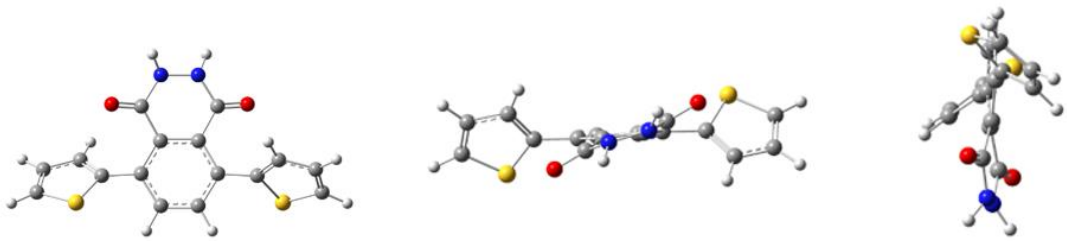

Figure 3.15 Confomations of T_2B-Lum from side view [35]

3.4. Electrochemistry of Compound

Cyclic voltammetry and square wave potential techniques, which are among the electrochemical methods, have been used in order to examine the redox properties of the corresponding compound. Firstly, electrolyte solution was prepared by dissolving 0.1 M TBAH electrolyte in acetonitrile in order to investigate the electrochemical properties of the compound. Button platinum (0.02 cm^2) WE, platinum wire CE and Ag/AgCl were used as RE. As seen in Figure 3.16, during the anodic scan of T_2B-Lum between 0.0 V and 2.0 V, three irreversible oxidation peaks were observed at 1.11 V (V_{onset} = 0.90 V), 1.68 V (V_{onset} = 1.48 V) and 1.76 V.

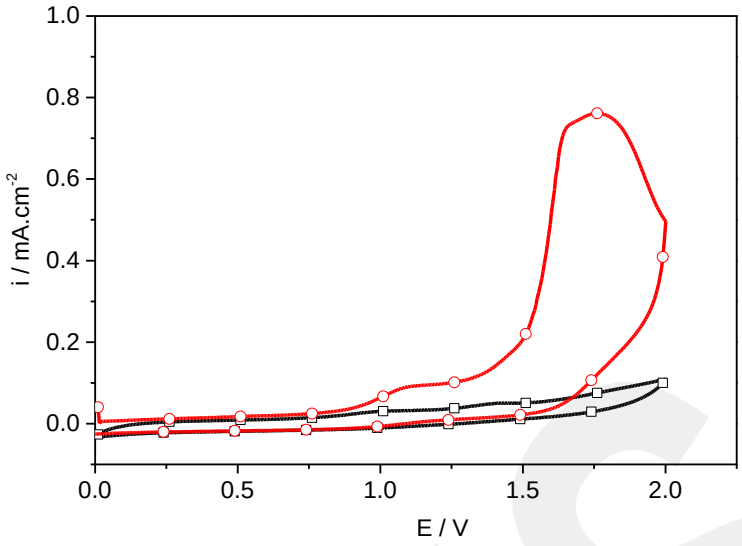

Figure 3.16 Cyclic voltammogram of T_2B-Lum (red line with circle) in 0.1 M TBAH/acetonitrile electrolyte solution between 0.0 V and 2.0 V at a scan rate of 100 mV/s (WE is Pt and black line with square is blank)

In Figure 3.17 (a), voltammogram shows the reduction of oxygen to the superoxide anion. While signal was not observed between 0.0 V and -1.3 V in inert environment, a reduction signal was observed at -1.05 V in open air environment due to dissolved oxygen in the solution. Figure 3.17 (b) shows the CL reaction of T_2B-Lum with superoxide anion when -1.05 V (2 s, the formation of superoxide anion) and 0.0 V (5 s) are applied at intervals.

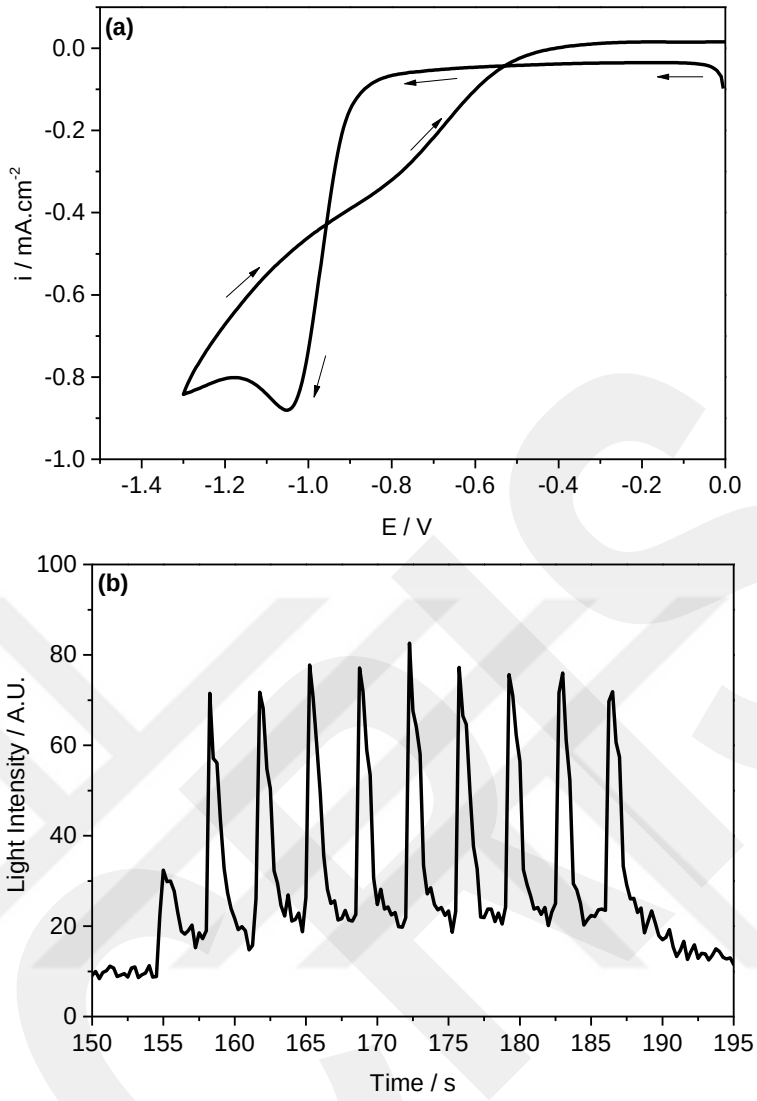

Figure 3.17 (a) Cyclic voltammogram of T_2B-Lum in 0.1 M TBAH/acetonitrile electrolyte solution under ambient condition (no inert atmosphere) and (b) the CL intensity of T_2B-Lum when various potentials (-1.05 V for 2s and 0.0 V for 5 s) are applied

In order to understand whether the CL radiation is caused by the reduced oxygen, the electrolysis cuvette was firstly purged with an inert gas to remove the dissolved oxygen in the electrolyte solution. Then, CL radiation was followed by applying an external potential of -1.05 V, formation of superoxide anion, to the system. As can be seen in Figure 3.18 (a), at the first stage, no signal was observed due to absence of oxygen in the solution. After removing inert gas from the solution, oxygen in the environment starts to dissolve in the electrolyte solution and reduced on the WE surface due to

applied potential of -1.05 V. Then, a signal was observed and its intensity steadily increases as a function of dissolved oxygen in the medium. The related study proves that reduced oxygen leads to the CL radiation. In addition, the decay curve of the CL radiation obtained is given in Figure 3.18 (b).

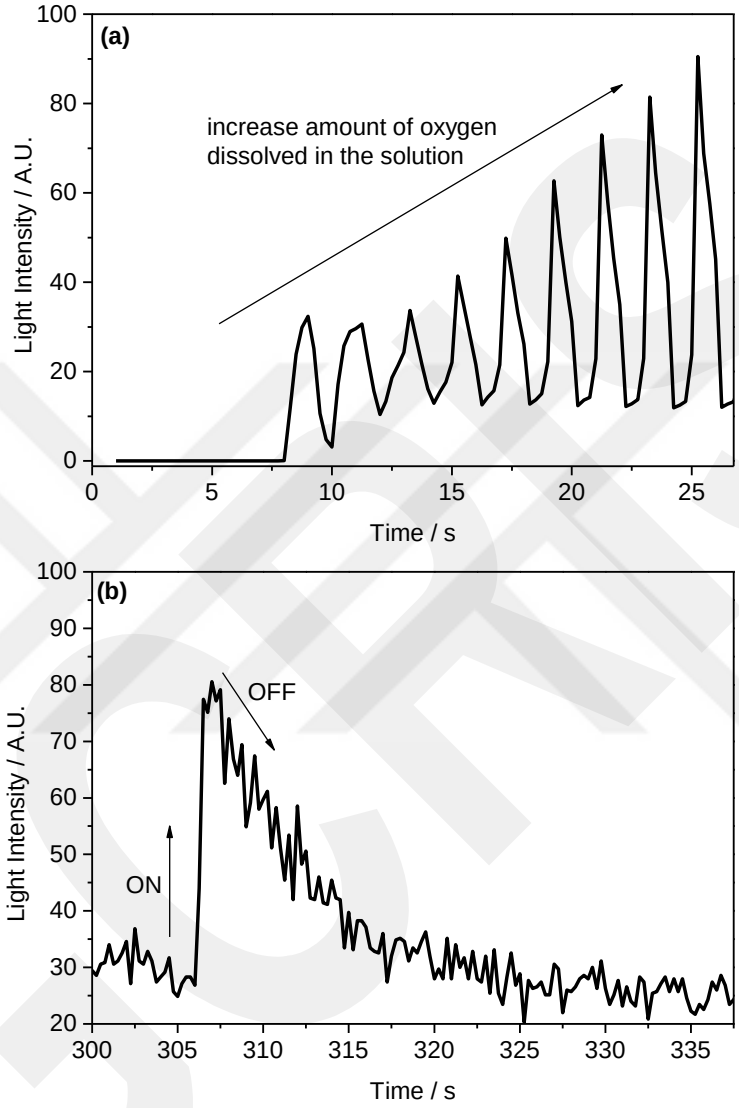

Figure 3.18 (a) The change observed in the radiation after the applied potentials (-1.05 V and 0.0 V) as a result of the displacement of the inert atmospheric pressure with the open air pressure in the 0.1 M TBAH/acetonitrile solution containing T_2B-Lum, (b) the decay curve of this radiation as a function of time.

3.5. CL Measurements of Compound

For CL measurements, a stopped-flow injection system combined with PMT was used. All the working solutions to be tested were freshly prepared. Distilled water was used to dilute H_2O_2, metal cations and blood solutions. $NaOH_{(aq)}$ solution was used for the dilution of luminol and hemin samples. T_2B-Lum was kept under $Ar_{(g)}$ in the refrigerator and also its solutions were protected from light and stored in refrigerator. Firstly, the CL intensity of compounds was examined against different oxidants in alkaline solutions. $KMnO_4$, $K_2Cr_2O_7$ and H_2O_2 were used as oxidants. CL intensities of T_2B-Lum and luminol with different oxidants (1.0×10^{-3} M) were given in Figure 3.19 and it was observed that H_2O_2 was the most effective oxidant for CL reaction of T_2B-Lum and luminol.

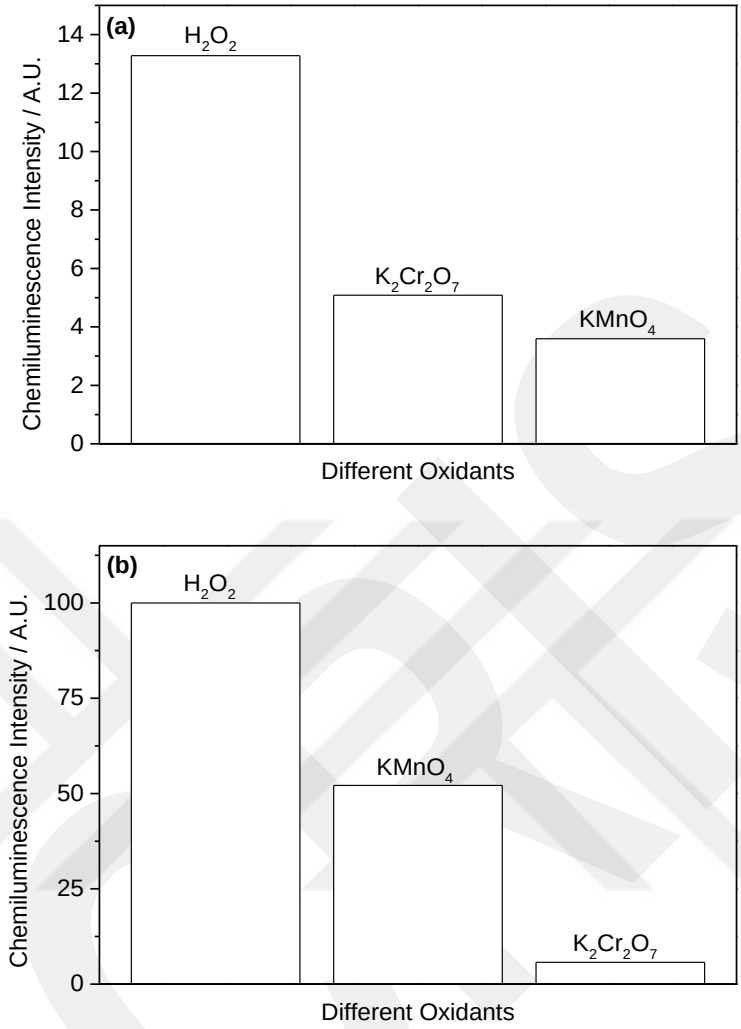

Figure 3.19 The CL intensity of 1.0×10^{-6} M (a) T_2B-Lum and (b) luminol in 0.1 M $NaOH_{(aq)}$ with 1.0×10^{-3} different oxidants

Then, the CL intensities of the T_2B-Lum and luminol were investigated against hydrogen peroxide at different concentrations in basic medium. As can be seen in Figure 3.20, the intensity of CL radiation changed depending on the hydrogen peroxide concentration as expected. It has been decided that it will continue to work with 1.0×10^{-3} M H_2O_2.

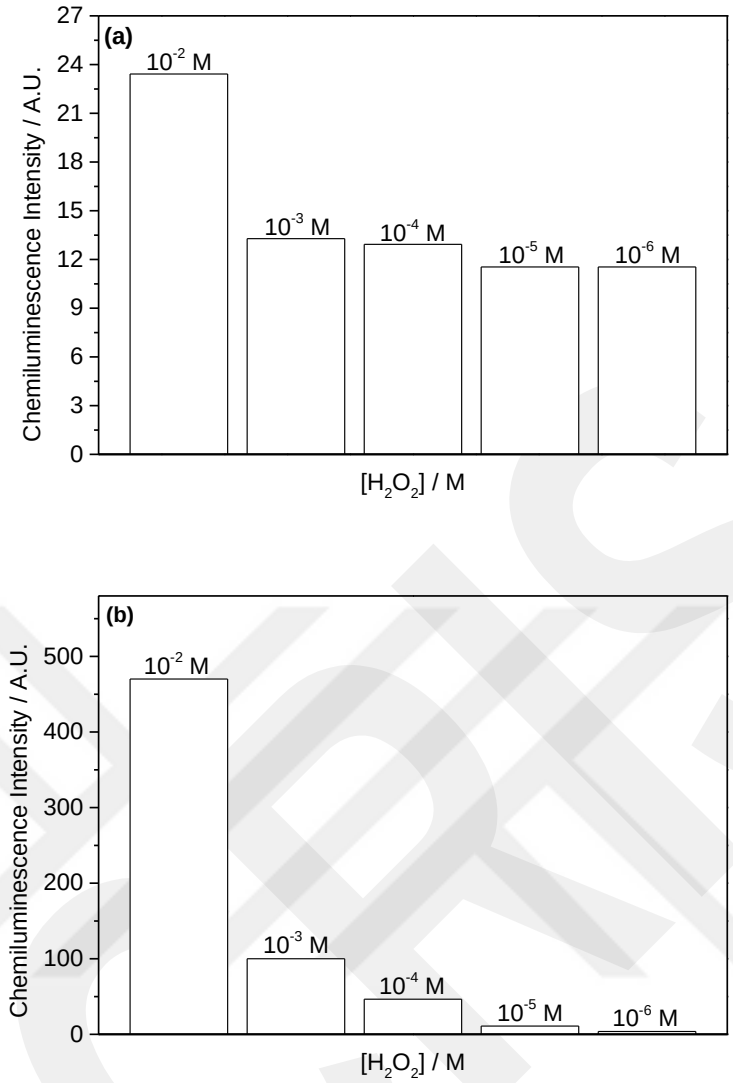

Figure 3.20 The CL intensity of 1×10^{-6} M (a) T_2B-Lum and (b) luminol in 0.1 M $NaOH_{(aq)}$ with different H_2O_2 concentrations

The proposed CL radiation mechanism for T_2B-Lum is given in Figure 3.21. The bridge established by the peroxides between the carbonyl groups in the pyridazine ring. This bridge causes the existing ring to be stretched too much and irreversibly broken. Released energy is observed as radiation in the visible region.

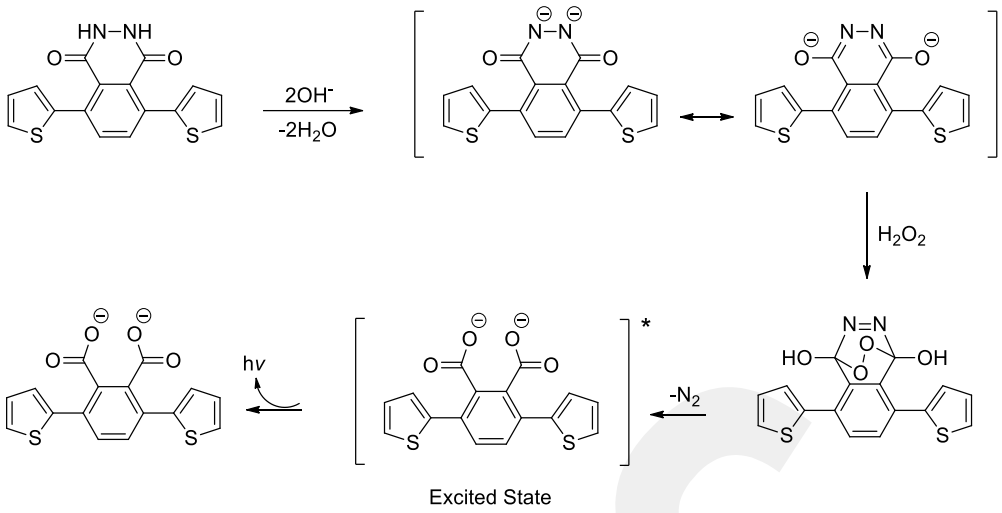

Figure 3.21 The proposed CL radiation mechanism for T_2B-Lum

After CL reaction of T_2B-Lum with hydrogen peroxide, it was checked whether this reaction was catalyzed in the presence of metal ions. The CL intensity of T_2B-Lum and luminol with H_2O_2 in an alkaline environment was examined in the absence (Figure 3.22 (a)) and presence (Figure 3.22 (b)) of Fe^{3+} catalyst. As can be seen in Figure 3.22, when Fe^{3+} catalyst is not used, CL intensity is very pale. On the other hand, the CL intensity increased sharply in the presence of Fe^{3+} ion, which confirms the catalytic role of Fe^{3+} ion in CL reaction.

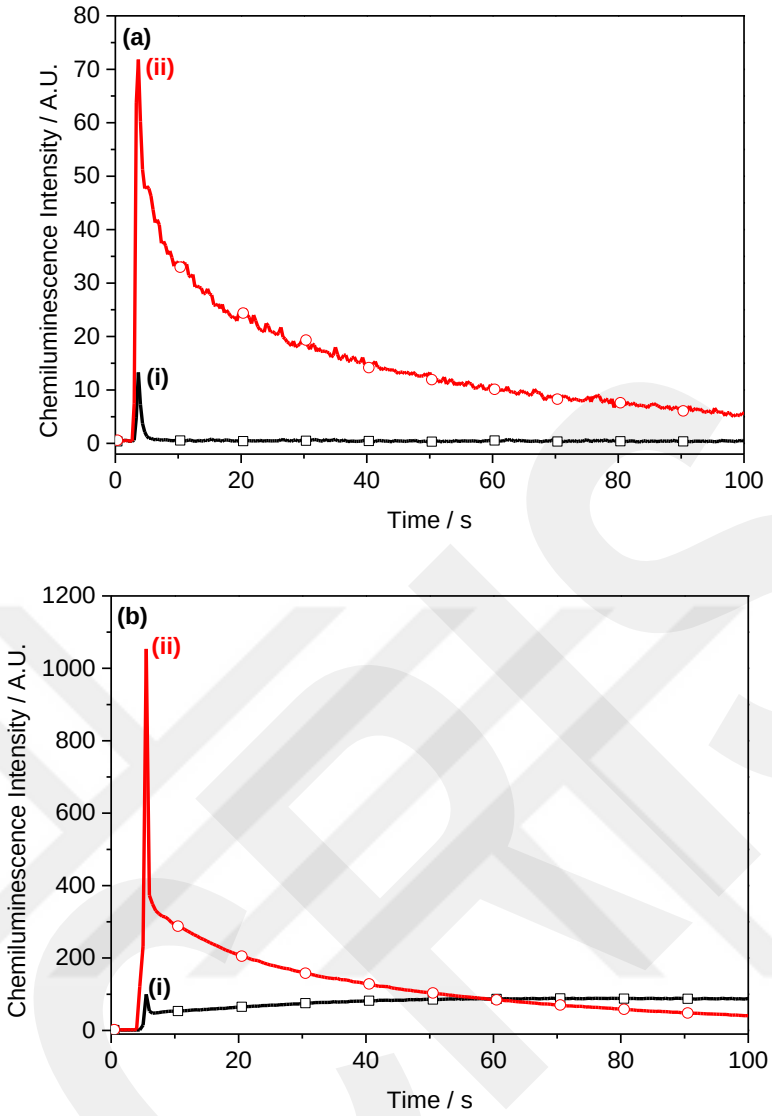

Figure 3.22 The CL intensity of 1.0×10^{-6} M (a) T_2B-Lum and (b) luminol with 1.0×10^{-3} M H_2O_2 in 0.1 M $NaOH_{(aq)}$ in the (i) absence (black lines with square) and (ii) presence of Fe^{3+} catalyst (red lines with circle)

Studies were repeated with various metal ions to investigate the effect of metal ions on CL intensity. As shown in Figure 3.23, it has been observed that the T_2B-Lum showed high CL intensity with copper metal ion. Luminol showed high CL intensity with aluminum metal ion.

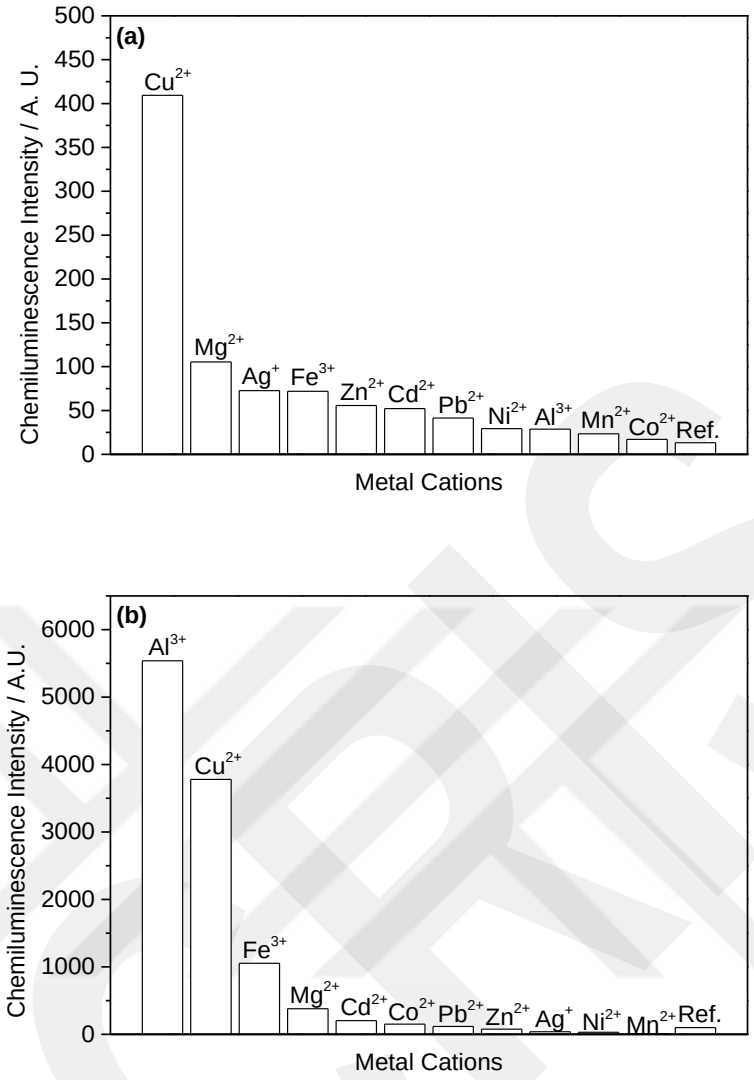

Figure 3.23 The CL intensity of 1.0×10^{-6} M (a) T_2B-Lum and (b) luminol in 0.1 M $NaOH_{(aq)}$ with 1.0×10^{-3} M H_2O_2 in the presence of the different metal cation concentrations

After observing this sensitivity, measurements were repeated for different copper concentrations as seen in Figure 3.24. As expected, it was observed that an increase in the copper ion concentration results in higher CL intensities of T_2B-Lum and luminol.

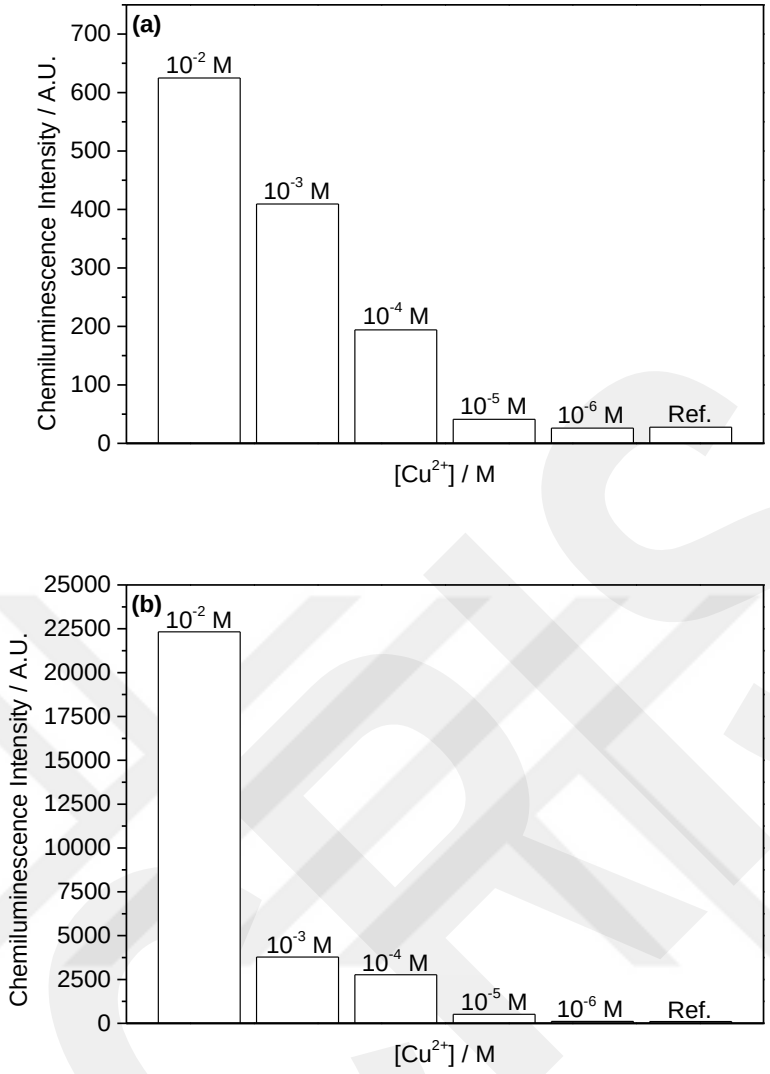

Figure 3.24 The CL intensity of 1.0×10^{-6} M (a) T_2B-Lum and (b) luminol in 0.1 M $NaOH_{(aq)}$ with 1.0×10^{-3} M H_2O_2 in the presence of the different Cu^{2+} ion concentrations

The CL intensities of the T_2B-Lum and luminol against different iron ions concentrations were also measured in order to examine the potential use of T_2B-Lum in blood diagnosis in forensic science (see Figure 3.25). High concentration of Fe^{3+} ion leads to intense CL emission of T_2B-Lum and luminol. Even at low concentration, the CL intensities were measured by PMT.

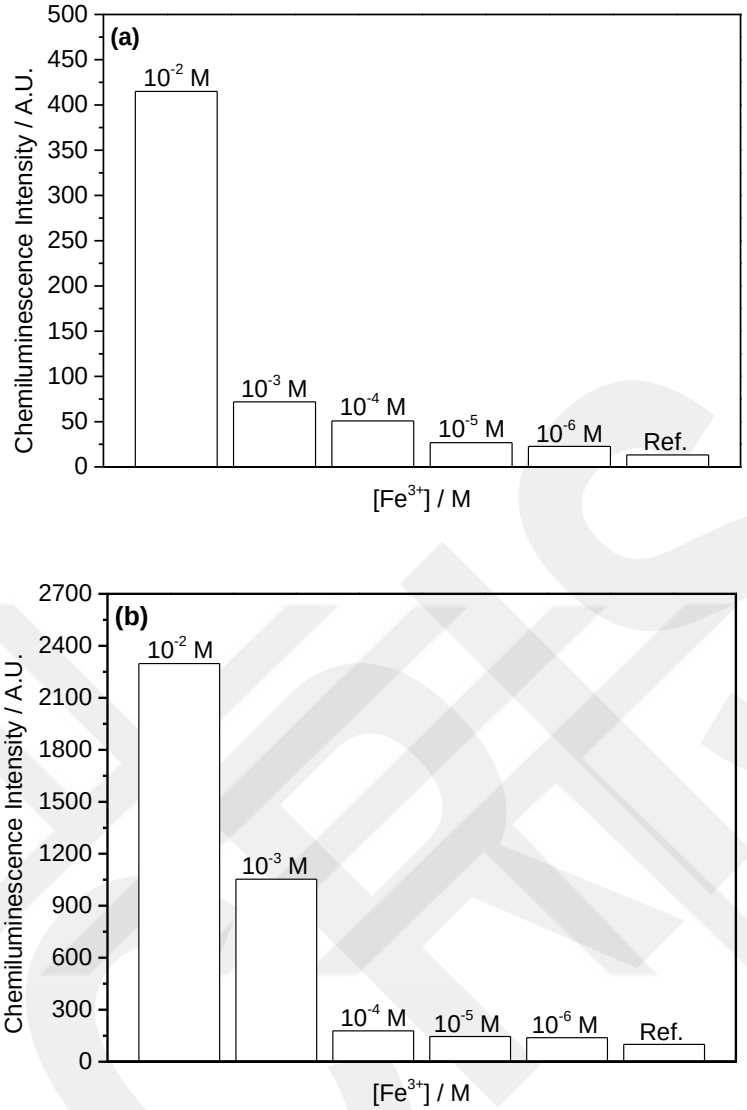

Figure 3.25 The CL intensity of 1.0×10^{-6} M (a) T_2B-Lum and (b) luminol in 0.1 M $NaOH_{(aq)}$ with 1.0×10^{-3} M H_2O_2 in the presence of the different Fe^{3+} ion concentrations

Since T_2B-Lum reacts against the iron ion, it has been wondered whether it will react to the iron ion in the blood. Therefore, measurements were made using a compound that called hemin, whose structure resembles hemoglobin. Figure 3.26 shows the CL intensity of T_2B-Lum against different hemin concentrations.

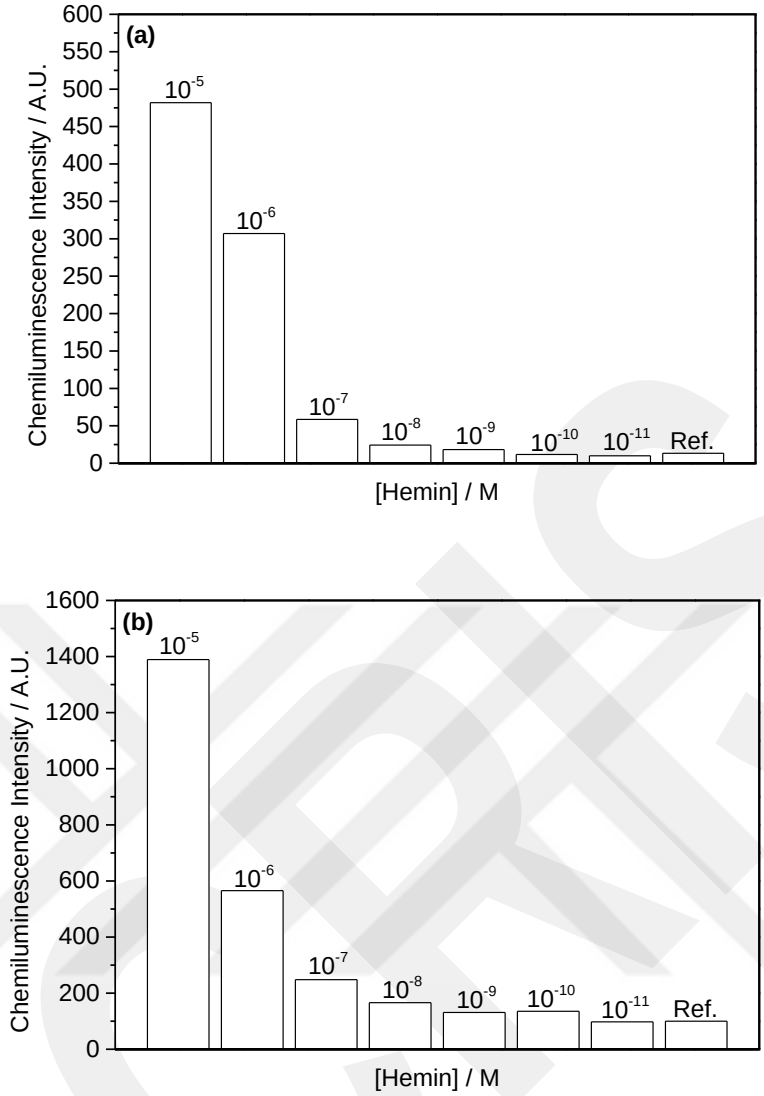

Figure 3.26 The CL intensity of 1.0×10^{-6} M (a) T_2B-Lum and (b) luminol in 0.1 M $NaOH_{(aq)}$ with 1.0×10^{-3} M H_2O_2 in the presence of the different hemin concentrations

Due to the sensitivity of the T_2B-Lum and luminol to hemin samples, blood samples were also studied in order to observe a similar sensitivity in blood samples. The blood was diluted with water in different proportions. As seen in Figure 3.27, it has been observed that CL radiation occurs with the help of PMT even at high dilution of 1 to 50,000. Approximately 1 ml of blood contains 0.5 mg of iron [36]. This means that the iron concentration in the blood is approximately 8.9×10^{-3} M. Blood diluted with water for 1:500 ratio containing approximately 1.8×10^{-5} M iron ions. CL intensity was measured with the help of PMT up to a concentration value of 1.8×10^{-7} M.

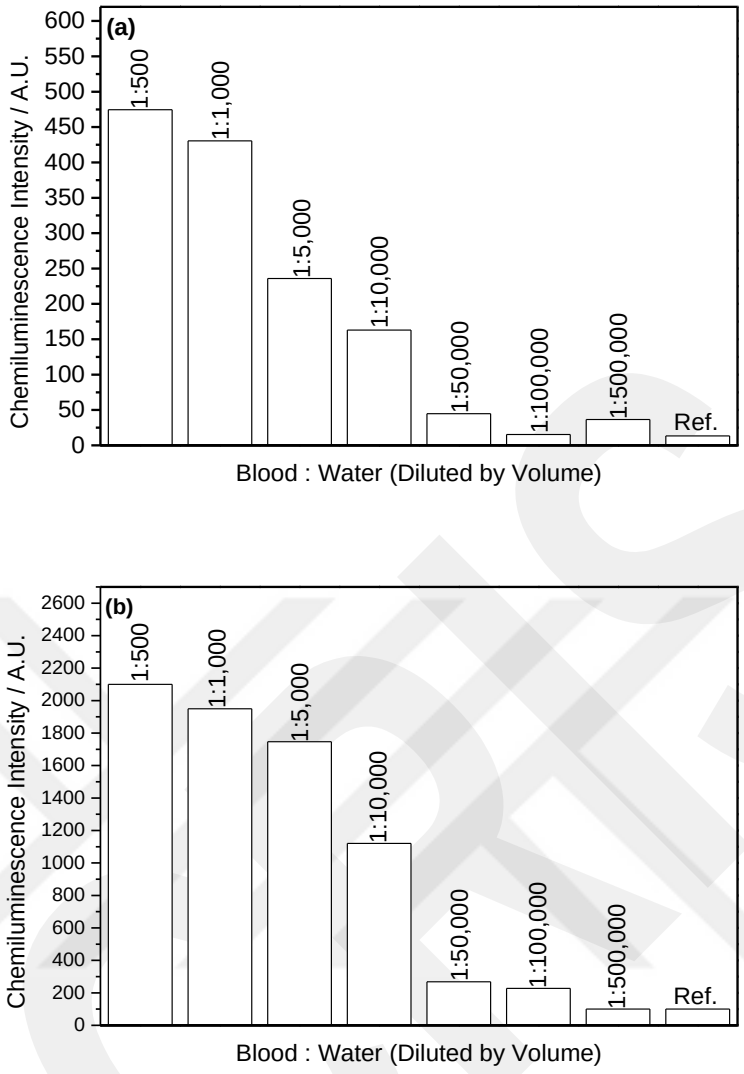

Figure 3.27 The CL intensity of 1.0×10^{-6} M (a) T_2B-Lum and (b) luminol in 0.1 M $NaOH_{(aq)}$ with 1.0×10^{-3} M H_2O_2 in the presence of the Fe^{3+} ion in blood concentrations diluted with different water volumes

In order to compare the effect of luminol and T_2B-Lum in CL measurements, it will be useful to provide a table with numerical values as well as a graphical representation. Table 3.4 (a) shows the CL intensity against different metal ions and (b) the coefficient at which different metal ions increase the CL intensity. Table 3.5 (a) shows the CL intensity against different hemin concentrations and (b) the coefficient at which different hemin concentrations increase the CL intensity. Table 3.6 (a) shows the CL intensity against different blood:water volume dilutions and (b) the coefficient at which different blood:water volume dilutions increase the CL intensity.

Table 3.4 (a) The CL intensity (b) increasing coefficient of CL intensity for 1.0×10^{-3} M T_2B-Lum and luminol in 0.1 M $NaOH_{(aq)}$ in the presence of 1.0×10^{-3} M H_2O_2 and 1.0×10^{-3} M different metal ions

	(a)		**(b)**	
	T_2B-Lum	Luminol	T_2B-Lum	Luminol
Reference	13.3	100	×1.0	×1.0
Ag^{+}	72.6	37.5	×5.5	×0.4
Al^{3+}	28.7	5539	×2.1	×55.4
Cd^{2+}	52.1	202.9	×3.9	×2.0
Co^{2+}	17.0	151.8	×1.3	×1.5
Cu^{2+}	409.4	3778.8	×30.8	×37.8
Fe^{3+}	71.8	1053.7	×5.4	×10.5
Mg^{2+}	105.4	379.6	×7.9	×3.8
Mn^{2+}	23.4	10.2	×1.7	×0.1
Ni^{2+}	29.4	31.5	×2.2	×0.3
Pb^{2+}	41.5	116.6	×3.1	×1.2
Zn^{2+}	55.7	76.3	×4.2	×0.8

Table 3.5 (a) The CL intensity (b) increasing coefficient of CL intensity for 1.0×10^{-3} M T_2B-Lum and luminol in 0.1 M $NaOH_{(aq)}$ at different hemin concentrations with 1.0×10^{-3} M H_2O_2

	(a)		**(b)**	
	T_2B-Lum	Luminol	T_2B-Lum	Luminol
Reference	13.3	100	×1.0	×1.0
10^{-5} M	482	1389.4	×36.2	×13.9
10^{-6} M	3067	565.6	×23	×5.7
10^{-7} M	58.6	248.2	×4.4	×2.5
10^{-8} M	24.3	166.2	×1.8	×1.7
10^{-9} M	18.3	131	×1.4	×1.3
10^{-10} M	11.6	135.2	×0.9	×1.4
10^{-11} M	10	97.8	×0.7	×1.0

Table 3.6 (a) The CL intensity (b) increasing coefficient of CL intensity for 1.0×10^{-3} M T_2B-Lum and luminol in 0.1 M $NaOH_{(aq)}$ at different blood:water volume dilutions with 1.0×10^{-3} M H_2O_2

	(a)		**(b)**	
	T_2B-Lum	Luminol	T_2B-Lum	Luminol
Reference	13.3	100	×1.0	×1.0
$1 : 5\times10^{2}$	474.5	2038.7	×35.6	×20.4
$1 : 1\times10^{3}$	430.4	1933.8	×32.4	×19.3
$1 : 5\times10^{3}$	236	1746.4	×17.7	×17.5
$1 : 1\times10^{4}$	163	1120	×12.3	×11.2
$1 : 5\times10^{4}$	44.7	268.3	×3.4	×2.7
$1 : 1\times10^{5}$	15.3	227.7	×1.1	×2.3
$1 : 5\times10^{5}$	36.5	100	×2.7	×1.0

3.6. Ion Recognition Property of T_2B-Lum

The fluorescence intensity effect of the compound was observed against many metal ions. Ag^{+} and Zn^{2+} ions increased the fluorescence intensity of the T_2B-Lum. T_2B-Lum was not sensitive to some metal ions (Cd^{2+}, Fe^{3+}, Li^{+}, Mg^{2+}, Mn^{2+} and Ni^{2+}). Co^{2+} metal ions quenched a little bit and Cu^{2+} (green line with triangle) metal ions quenched almost completely as shown in Figure 3.28 and Figure 3.29.

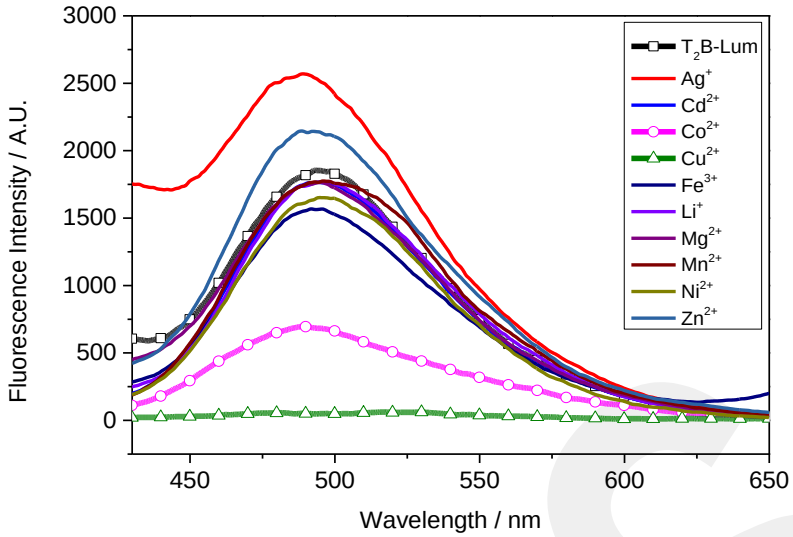

Figure 3.28 Fluorescence spectra of T_2B-Lum (1.0×10^{-5} M in acetonitrile) upon addition of various metal ions (0.02 M in water) (λ_{exc} = 350 nm). Black line with square shows the reference.

The fluorogenic effect of the compound against different concentrations of copper ion is shown in Figure 3.29. As the copper concentration increased as expected, T_2B-Lum quenched its fluorescence effect.

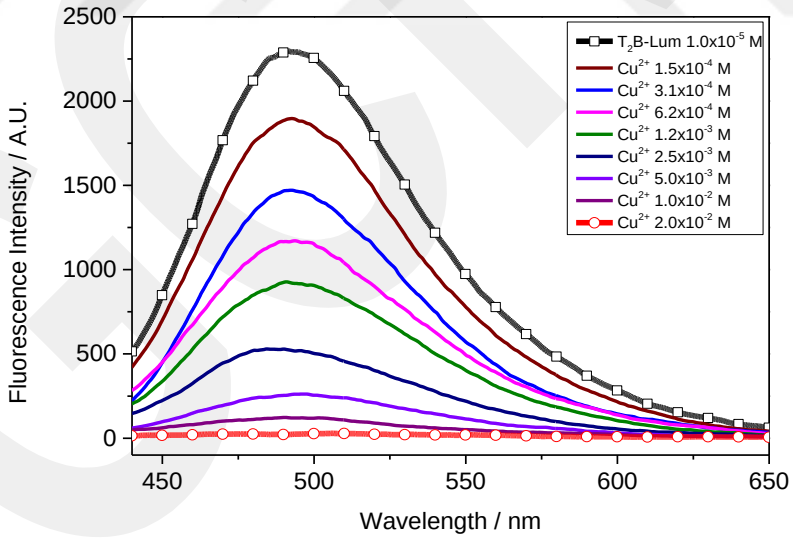

Figure 3.29 Fluorescence spectra of T_2B-Lum (1.0×10^{-5} M in acetonitrile) upon addition of different copper metal ion concentration in acetonitrile (λ_{exc} = 350 nm)

Figure 3.30 shows the bluish-green emission of T_2B-Lum against metal ions in UV light.

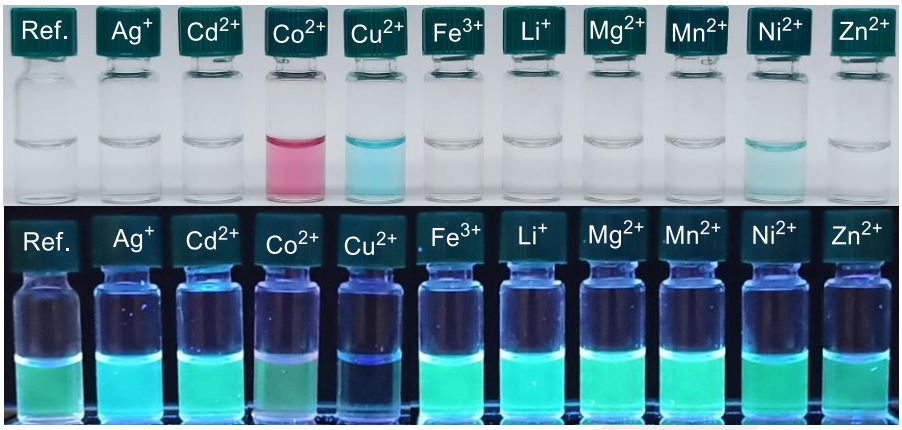

Figure 3.30 Fluorogenic response of T_2B-Lum (1.0×10^{-5} M) to various metal ions (0.02 M) under daylight and UV light (365 nm)

As seen in Figure 3.31, as the Cu^{2+} ion concentration in T_2B-Lum increases, the fluorescence intensity value of T_2B-Lum decreases.

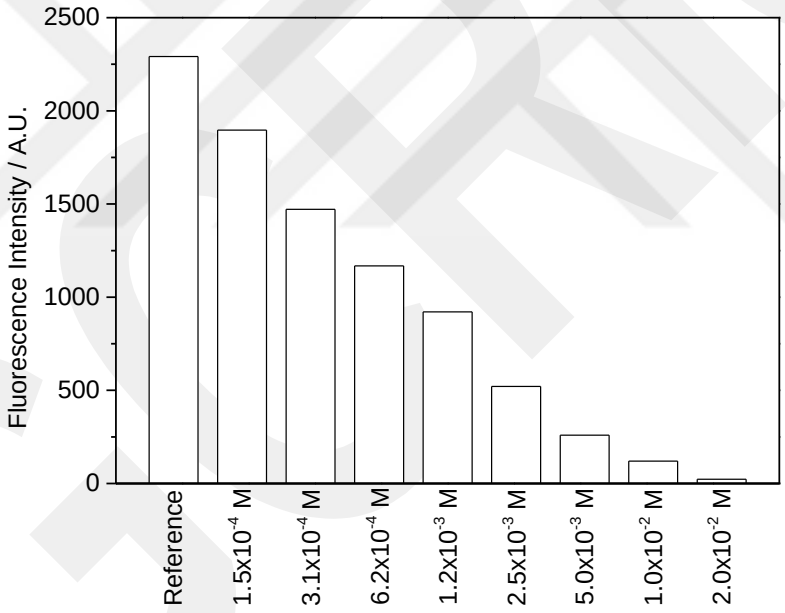

Figure 3.31 Fluorescence intensity of T_2B-Lum with increase in Cu^{2+} ion concentration

According to the Figure 3.32, the limit of detection value of the substance showing sensitivity to copper ions was accepted as 2.2×10^{-3} M.

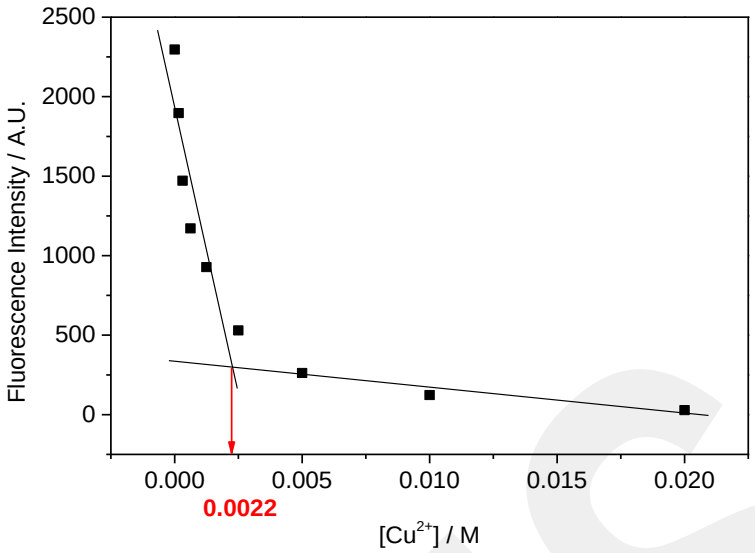

Figure 3.32 Estimated limit of detection value and decreasing of fluorescence intensity for T_2B-Lum solution (1.0×10^{-5} M in acetonitrile) with increasing total copper concentration in the solution

The Stern-Volmer relationship provides information about the kinetics of an intermolecular deactivation process. K_{sv} is the quenching rate constant for Stern-Volmer approach. The rate of quenching the emission of T_2B-Lum by the copper ion was found to be 1757.7 L.mol^{-1} in Figure 3.33.

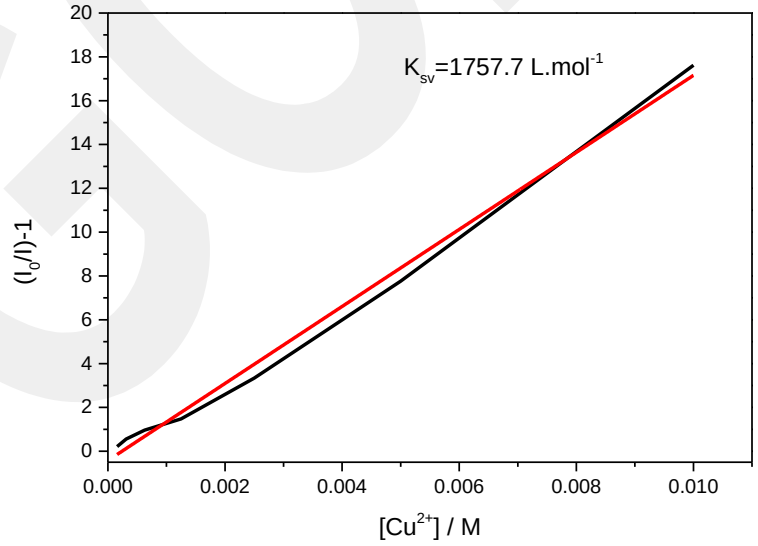

Figure 3.33 Stern-Volmer plot of T_2B-Lum against the Cu^{2+} ion

CHAPTER 4

CONCLUSION

In this thesis, a trimeric chemiluminescent compound called T_2B-Lum was studied. Structural confirmation of the corresponding synthesized compound were carried out using NMR, HRMS, and FTIR. Considering the analysis results, it is seen that T_2B-Lum was synthesized successfully. Then, UV and fluorescence measurements were taken to investigate the optical properties of the compound. T_2B-Lum exhibits two absorption bands at 262 and 330 nm in DCM and emits green light at 495 nm when excited. The QY of T_2B-Lum was calculated as 15.11% in DCM when considering the luminol QY is 100%

After, the CL properties of T_2B-Lum were investigated. The CL reactions of T_2B-Lum was investigated in alkaline solution with different oxidants such as H_2O_2, $KMnO_4$, $K_2Cr_2O_7$. H_2O_2 determined as appropriate oxidizers. The appropriate concentration of H_2O_2 was determined as 1.0×10^{-3} M. Subsequently, it was observed whether the CL intensity of T_2B-Lum catalyzed metal ions or not. Metal ions such as Al^{3+}, Ag^{+}, Cd^{3+}, Cu^{2+}, Co^{3+}, Fe^{3+}, Mg^{3+}, Mn^{2+}, Ni^{3+}, Pb^{3+} and Zn^{3+} were used in metal ion analyzes. Especially, Cu^{2+} ion was catalyzed the CL intensity of T_2B-Lum. It was also observed that the chemiluminescent emission was catalyzed by Fe^{3+} ions. In addition, hemin is a compound structure similar to hemoglobin which is found in the blood and this compound used in analyzes. It has been observed that the T_2B-Lum responds approximately until 1.0×10^{-11} M for hemin. After the sensitivity of T_2B-Lum to hemin was observed, the studies were continued with blood. The blood was diluted with water to a ratio of 1:500 to 1:50,000 and T_2B-Lum was observed to respond in this range.

In addition, the ion recognition property of T_2B-Lum was investigated.

As a result of this study, it has been proved that the substance can be used as a fluorogenic probe especially copper metal against to other metal ions such as Ag^{+}, Cd^{2+}, Co^{2+}, Fe^{3+}, Li^{+}, Mg^{2+}, Mn^{2+}, Ni^{2+} and Zn^{2+}. The detection value limit of the compound was accepted as 2.2×10^{-3} M.

REFERENCES

[1] B.W. Darvell, "Radiography" in *Materials Science for Dentistry*, 10th ed. L. Overend, Ed. United Kingdom: Woodhead Publishing, 2018, pp. 665–698.

[2] T. L. Brown, Jr. H. E. LeMay, B. E. Bursten, C. J. Murphy, P. M. Woodward, M. W. Stoltzfus, "Electronic Structure of Atoms" in *Chemistry The Central Science*, 13th ed. A. Jaworski, Ed. United States of America: Pearson Education, 2014, pp. 212-255.

[3] G. B. Nair, S. J. Dhoble, "The Fundamentals and Applications of Light-Emitting Diodes". *The Revolution in the Lighting Industry*, vol. 30, issue 8, pp. 1167-1175, May 2015.

[4] R. Capelletti, "Luminescence" in *Encyclopedia of Condensed Matter Physics*. F. Bassani, G. L. Liedl, P. Wyder, Eds. Amsterdam: Elsevier Acad. Press, 2005, pp. 178-189.

[5] T. H. Fereja, A. Hymete, T. Gunasekaran, "A Recent Review on Chemiluminescence Reaction, Principle and Application on Pharmaceutical Analysis". *ISRN Spectroscopy*, vol. 2013, pp. 1-12, Sep 2013.

[6] A. Beall, "See the northern lights or aurora borealis: Follow this easy guide". Internet: https://www.newscientist.com/article/mg24432590-500-see-the-northern-lights-or-aurora-borealis-follow-this-easy-guide/, [04 December 2019]

[7] National Geographic, "Pictures: Glowing Blue Waves Explained". Internet: https://www.nationalgeographic.com/news/2012/3/120319-glowing-waves-ocean-blue-bioluminescent-plankton-science/, 19 March 2012 [04 December 2019]

[8] "Bioluminescent Animals & Plants-Biochemical Beacons". Internet: https://blog.indigoinstruments.com/bioluminescence-biological-light-beacons/ 01 August 2017 [22 July 2019].

[9] A.M. Garcia-Campana, W.R.G. Baeyens, M. Roman-Ceba, “Historical Evolution of Chemiluminescence” in *Chemiluminescence in Analytical Chemistry*. A.M. Garcia-Campana, W.R.G. Baeyens, Eds. United State of America: Marcel Dekker, Inc., 2001, pp. 2-12.

[10] F. Barni, S. W. Lewis, S. Berti, G.M. Miskelly, G. Lago, "Forensic application of the luminol reaction as a presumptive test for latent blood detection". *Talanta*, vol. 72, issue 3, pp. 896–913, Jan 2007.

[11] K. E. Haapakka, "The mechanism of the cobalt(II)-catalyzed electro-generated chemiluminescence of luminol in aqueous alkaline solution". *Analytica Chimica Acta*, vol. 141, pp. 263–268, Sep 1982.

[12] D. F. Roswell, E. H. White, “The chemiluminescence of luminol and related hydrazides”. *Methods in Enzymology*, vol. 57, pp. 409–423, 1978.

[13] M. M. Richter, “Electrochemiluminescence” in Optical Biosensors, 2nd ed. F. S. Ligler, C. R. Taitt, Eds. Amsterdam: Elsevier, 2008, pp. 317–384.

[14] K. Hiramoto, E. Villani, T. Iwama, K. Komatsu, S. Inagi, K. Inoue, Y. Nashimoto, K. Ino, H. Shiku, "Recent Advances in Electrochemiluminescence-Based Systems for Mammalian Cell Analysis". *Micromachines*, vol. 11, issue 5, pp. 1-23, May 2020.

[15] Y. S. Choudhary, L. Jothi, G. Nageswaran, "Electrochemical Characterization" in *Spectroscopic Methods for Nanomaterials Characterization*, vol. 2. S. Thomas, R. Thomas, A. K. Zachariah, R. K. Mishra, Eds. Amsterdam: Elsevier, 2017, pp. 19–54.

[16] Cyclic Voltammetry Explained: Basic Principles & Set Up, Internet: https://www.ossila.com/pages/cyclic-voltammetry, Ossila, [20 December 2020].

[17] P. Khan, D. Idrees, M. A. Moxley, J. A. Corbett, F. Ahmad, G. von Figura, W. S. Sly, A. Waheed, M.I. Hassan, "Luminol-Based Chemiluminescent Signals: Clinical and Non-clinical Application and Future Uses". *Applied Biochemistry and Biotechnology*, vol. 173, issue 2, pp. 333–355, May 2014.

[18] C. A. Marquette, L. J. Blum, "Applications of the luminol chemiluminescent reaction in analytical chemistry". *Analytical and Bioanalytical Chemistry*, vol. 385, issue 3, pp. 546–554, May 2006.

[19] R. Rogiski da Silva, B. C. Agustini, A. L. Lopes da Silva, H. R. Frigeri, "Luminol in the forensic science". *Journal of Biotechnology and Biodiversity*, vol. 3, issue 4, pp. 172-177, Nov 2012.

[20] T. Harris, "How Luminol Works" Internet: https://science.howstuffworks.com /luminol1.htm, [20 December 2020].

[21] D. Asil, A. Cihaner, A. M. Önal, "Electropolymerization and ion sensitivity of chemiluminescent thienyl systems". *Electrochimica Acta*, vol. 54, issue 26, pp. 6740–6746, Nov 2009.

[22] N. Atılgan, F. Algı, A. M. Onal, A. Cihaner, "Synthesis and properties of a novel redox driven chemiluminescent material built on a terthienyl system". *Tetrahedron* vol. 65, pp. 5776–5781, Jul 2009.

[23] D. Asil, A. Cihaner, F. Algı, A. M. Onal, "A Diverse-Stimuli Responsive Chemiluminescent Probe with Luminol Scaffold and Its Electropolymerization". *Electroanalysis*, vol. 22, issue 19, pp. 2254–2260, Jul 2010.

[24] A. Degirmenci, F. Algi, "Synthesis, chemiluminescence and energy transfer efficiency of 2,3-dihydrophthalazine-1,4-dione and BODIPY dyad". *Dyes and Pigments*, vol. 140, pp. 92-99, May 2017.

[25] M. Pamuk, F. Algi, "Incorporation of a 2,3-dihydro-1H-pyrrolo[3,4-d]pyridazine-1,4(6H)-dione unit into a donor–acceptor triad: synthesis and ion recognition features". *Tetrahedron Letters*, vol. 53, issue 52, pp. 7117–7120, Jan 2012.

[26] H. Yoshida, R. Nakao, H. Nohta, M. Yamaguchi, "Chemiluminescent properties of some luminol-related compounds". *Dyes and Pigments*, vol. 47, pp. 239-245, Dec 2000.

[27] J. Han, J. Jose, E. Mei, K. Burgess, "Chemiluminescent Energy-Transfer Cassettes Based on Fluorescein and Nile Red". *Angewandte Chemie International Edition*, vol. 46, pp. 1684–1687, Feb 2007.

[28] T. F. Jiao, Y. Y. Xing, J. X. Zhou, W. Wang, “Synthesis and Characterization of Some Functional Luminol Derivatives with Aromatic Substituted Groups”. *Advanced Materials Research*, vol. 197-198, pp. 606–609, Feb 2011.

[29] R. Nawaz, T. Rasheed, M. Bilal, S. Majeed, Z. Iqbal, T. Iqbal, F. Ali, "Luminol immobilized graphite electrode as sensitive electrochemiluminescent sensor for the detection of hydrogen peroxide". *Sensors International*, vol. 1, issue 10027, pp. 1-5, 2020.

[30] Chemistry LibreTexts, “How an FTIR Spectrometer Operates”, Internet: https://chem.libretexts.org/Bookshelves/Physical_and_Theoretical_Chemistry_Textbook_Maps/Supplemental_Modules_(Physical_and_Theoretical_Chemistry)/Spectroscopy/Vibrational_Spectroscopy/Infrared_Spectroscopy/How_an_FTIR_Spectrometer_Operates, [20 December 2020].

[31] P. Beauchamp, “Infrared Tables”. Spectroscopy Tables, Department of Chemistry, Cal Poly Pomona, California.

[32] A. M. Brouwer, "Standards for photoluminescence quantum yield measurements in solution (IUPAC Technical Report)". *Pure and Applied Chemistry*, vol. 83 issue 12, pp. 2213–2228, Jan 2011.

[33] J. R. Lakowicz, “Instrumentation for Fluorescence Spectroscopy” in *Principles of Fluorescence Spectroscopy*, 2nd ed. New York: Kluwer Academic/Plenum, 1999, pp. 52-53.

[34] A. Bukauskytė, R. Karpicz, R. Striela, L. Labanauskas, A. Gruodis, D. Peckus, R. Augulis, V. Gulbinas, “The Influence of Substituents of Perylenediimides on Their Spectroscopic Properties”. *Journal of Luminescence*, vol. 195, pp. 252–258, Mar 2018.

[35] E. Demir Arabacı, E. Yıldırım, 2021 [Unpublished results].

[36] V. Reddy K, S. Shastry, M. Raturi, P. Baliga B, “Impact of Regular Whole-Blood Donation on Body Iron Stores”. *Transfusion Medicine and Hemotherapy*, vol. 47, issue 1, pp. 1-5, May 2019.